Implementing Optical Field Analog Computation with Bacteriorhodopsin: A Feasibility Study

A Thesis

Presented for the

Master of Science Degree

The University of Tennessee, Knoxville

Quentin A. Browne

December 1996

Acknowledgments

First and foremost I want to thank GOD for giving me the strength and courage to persevere to the end and holding fast to his promise in Isaiah 40:31 “But they that wait upon the LORD shall renew their strength; they shall mount up with wings as eagles; they shall run, and not weary; and they shall walk and not faint” (KJV).

I also wish to thank my advisor, Dr. Bruce Maclennan, for his patience, guidance and support throughout this project. I also want to take this opportunity to express my gratitude to the other members of my committee, Dr. Michael Berry and Dr. Bradley Vander Zanden for serving on my committee.

I would also like to thank Dian Witter and David Stark for their time and talents in proofreading my rough drafts.

I would like to thank my fellow co-workers at Network Services. Their help and expertise made this project possible.

Finally, I would to thank all my family and friends who prayed for me, let us not dilute the power of prayer.

Abstract

This thesis describes the use of Bacteriorhodpsin (BR) to perform optical analog field computation, specifically, analog addition. Bacteriorhodpsin, a photoactive photocyclic protein, was modeled and simulated through four experimental setups. Combinations of two wavelengths, which were the peak absorption wavelengths for the two major states M and bR, made up the four experiments. The setups which combined two different wavelength were better suited to doing addition than the same-wavelength setups. We showed that the ratio of write to read time controls the slope of the approximately linear relation between the input and the output. Conversely, the read intensity determines the y-intercept of the line. By solving these (approximate) equations we were able to find read/write parameters that enable BR to perform analog addition, with the sum represented by the same power range as the inputs.

Contents

List of Figures

Chapter 1

INTRODUCTION

1.1 Motivation

Computer technology has advanced tremendously in the past decade. We now have processors with speeds that were unheard of ten years ago. Despite these great achievements, present day computers still cannot perform many of the most basic human cognitive processes, such as perception, association, sensory-motor coordination, and judgment of similarity [13]. This is because many of these cognitive functions require the flexible processing of large amounts of ambiguous, incomplete, or redundant information, including images, speech and natural language [14].

Artificial Intelligence (AI) was supposed to answer this problem but failed to deliver on its promises. AI has a “cognitive inversion”, meaning it does best what people do poorly and does poorly what people do best [11]. For example, AI has been successful in proving theorems, analyzing blood, and playing board games such as chess and checkers [11]. However, even our most powerful computers cannot accomplish day-to-day tasks like recognizing a face, or understanding spoken or written language, or maneuvering in and out of its environment.

Recognizing the limitations of existing AI technology has led to the development of a very different approach, called "the new AI" [11]. This approach falls under related ideas such as connectionism, artificial neural networks, flexible information processing, and emergent computation (see Maclennan for details). The new AI is the heart of the new information processing technology [11]. This technology comprises flexible computing ("intuitive information processing"), adaptive computing, and massively parallel computing [11].

The new information processing technology will be based on the way the brain works. The brain does not process information like conventional computers. Conventional information processing has narrow but deep computation, high precision (digital), and a small number of fast processors. The new AI, like the brain, will implement wide but shallow computation, low precision (analog), and use an extremely large number of possibly slow processors [12]. If a new technology cannot scale up to a million to a billion processors with a billion to a trillion connections, then it is not on the trajectory to the new information processing technology [12]. The new AI will allow us to make use of massively parallel computers (including neurocomputers), optical computers, molecular computation, and a new generation of analog computers. What these computational paradigms have in common is that they process massive amount of information in parallel. A computational system is said to be massively parallel if the number of processing elements is so large that it may conveniently be considered a continuous quantity [8].

1.2 Molecular and Optical Computing

Molecular computing is an emerging field that lies at the interface of chemical physics, biophysics, electrical engineering, and solid state science [1]. It involves the encoding, manipulation, and retrieval of information at a macromolecular level as opposed to current techniques [1]. There are significant advantages inherent in the use of biological molecules, either in their native form, or modified via chemical or mutagenic methods, as active components in molecular computing devices [1]. These advantages derive in large part from the natural selection process, and the fact that nature has solved through trial and error problems of a nature similar to those encountered in harnessing organic molecules to carry out logic, switching, and energy transducing functions [1].

Molecular and optical computers naturally have such large numbers of processing elements that they are considered continuous. Due to the enormous number of processors, these computers cannot be individually programmed so we have to think of them as one continuous quantity. Parallelism is not something new, but the "new AI" researchers are taking a different approach to it. Instead of thinking about the data separately they are examined as a field (i.e. a continuous, dense ensemble of information).

1.3 Field Computation

Field transformations are any operation on a field (scalar or vector), either to produce another field or to produce a new state of the field, which can be considered massively parallel if it operates on all the elements of the field in parallel [10]. For examples of field transformations see Figure 1.1. Field computers are computers that perform (in parallel) transformations on scalar fields (such as potential fields) and vector fields (such as gradient fields) [10]. Most field computers that are built today are for special purposes. One side effect of this research is to further the study on the hardware and software of a universal field computer.

1.4 Bacteriorhodopsin

Bacteriorhodopsin (BR) is a photoactive protein that has great potential in optical and molecular computing. BR is a unique biological molecule since it is the only protein found in nature in a crystalline membrane [4]. This crystalline membrane is called the purple membrane (PM), and BR is the sole protein component of

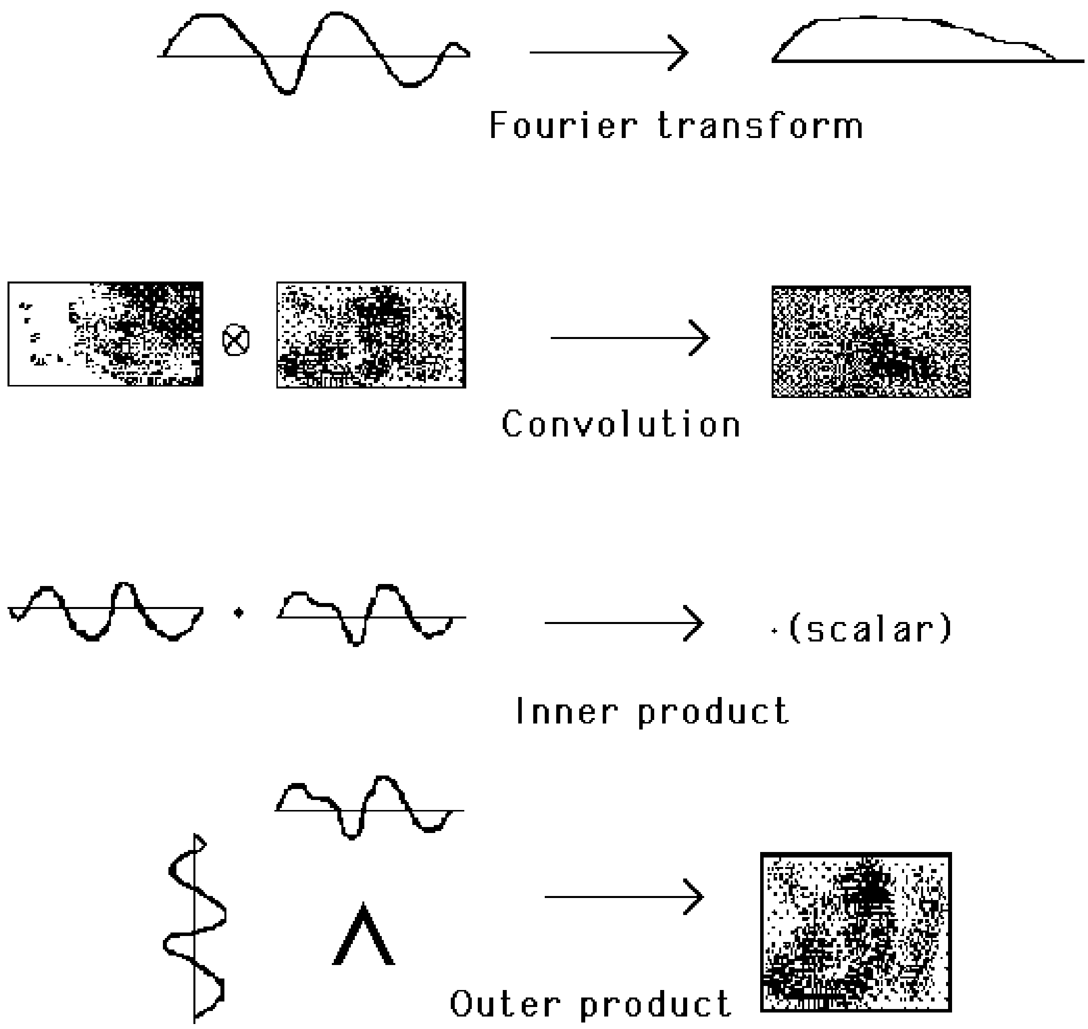

Figure 1.1: Examples of Field Transformation from [9]

this membrane produced by the bacterium Halobacterium halobium [4]. The bacterium thrives in salt marshes where the salt concentration is six times greater than that of seawater [6]. It is able to survive in the harsh conditions of high temperature and intense light in salt marshes by switching from respiration to photosynthesis. The physiological role of BR in the bacterium is to convert light energy into a proton gradient across the bacterial cell membrane generating a chemical and osmotic potential that serves as an alternate source of energy [4].

By absorbing visible light BR undergoes several structural transformations in a well-defined photocycle (see Figure 1.2). BR can photochemically cycle on the order of 10^6 times without any sign of fatigue (degradation in sensitivity) [2]. Figure 1.3 shows the absorption spectra of BR. In its resting (initial) state bR, BR has an absorption maximum of 570 nm. After the absorption of a photon it passes quickly through several intermediate states, then thermally relaxes to the M state. It has a lifespan in the M state of 10ms at ambient temperature, but it can be lengthened greatly with chemicals and genetic engineering. It can return to the initial state thermally or with a photoreaction response at a maximum absorption wavelength of 410nm.

Soviet scientists were the first to notice the potential of BR, believing it to be the computer breakthrough that would put them ahead of the United States [3]. BR has attracted such attention because of its potential in so many applications such as spatial light modulators (SLM), holographic associative memories, Fourier

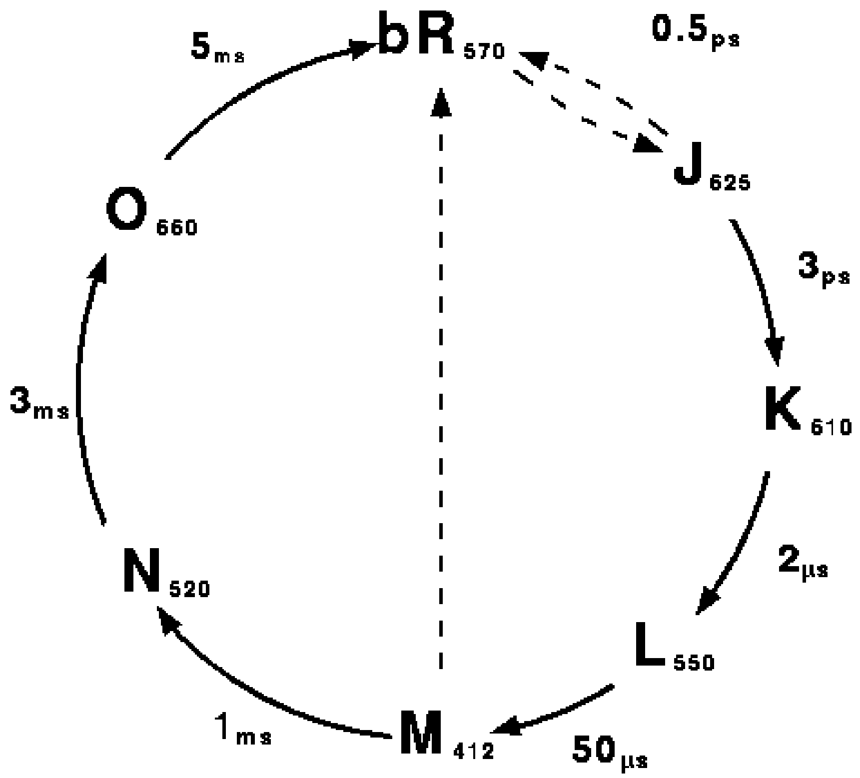

Figure 1.2: Photocycle of Bacteriorhodopsin. The dashed arrows indicate the photon driven process. The solid arrows show the thermal decay path. Modified from [4]

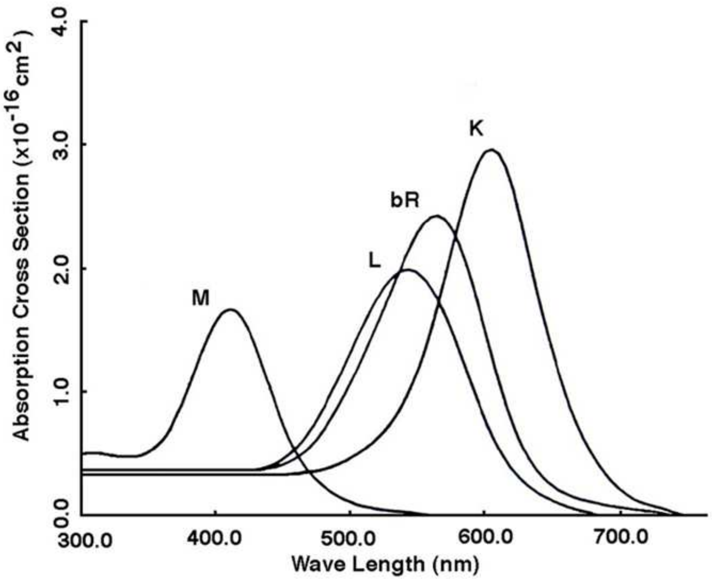

Figure 1.3: Absorption Spectra of Bacteriorhodopsin. From [4]

transform holographic associative memories, neural networks, 3-D optical memory, and random-access cache memory [2].

1.5 Objective

The viewpoint expressed in this thesis is based on the work of Dr. Bruce Maclennan. His insight and work in continuous computation laid the foundation for this project. Presently, BR is a hot topic of research but most of the work done with BR concentrates on using it in some discrete (digital) way. Our objective is to use BR in the way that it naturally operates. This thesis will discuss the implementation and results of simulating the use of bacteriorhodopsin to perform certain operations defined for field computers.

Chapter 2

The Simulation

It is surprising that a simulation software package is not currently available for analyzing Bacteriorhodopsin (BR) since it is popular. It was necessary to write a new simulation program.

By incorporating the theory of photochromism (the study of materials that change color with the absorption of light), optics, and some experimental data on BR characteristics, I came up with a working model. Originally, the model was made as simple as possible under ideal conditions. Then I proceeded to alter and upgrade the model to simulate realistic conditions the BR will experience.

2.1 BR Preparation

As stated in the introduction, the BR can be chemically and genetically enhanced. The BR used in the simulation model of this project was based on an actual genetically enhanced BR that has a longer life span for the M state. The light sensitivity of this BR variant was increased which resulted in a high M population, even at low light intensities [15].

BR can be incorporated into a number of water soluble polymers [6]. Polyvinyl alcohol (PVA), bovine gelatin, polyethylene glycol and methyl cellulose are all suitable matrices which form good quality, variable optical density thin films [6]. In theory, because BR is so versatile, the parameters such as optical density, light sensitivity, thickness, quantum yields and reading and recording wavelengths can vary to a wide degree. Therefore, it is possible to chemically or genetically engineer a physical BR to best fit the optimal researched simulation characteristics.

2.2 The Simulation Setup

The new simulation model of BR incorporates a two-state model. The two-state model consists of $bR \Rightarrow M$ and the $M \Rightarrow bR$ reactions. The life span of the intermediate states are so short they can be neglected. The simulation processed a small piece of BR in preparation for later extrapolation to a full sheet.

There were many variables and situations to consider for the simulation model. If all of them were examined, a functioning model would not have been possible. Some of the concern about the model accuracy was beyond the scope of this project, and would be better handled by some other discipline such as physics, engineering, or chemistry. The approach to the new simulation model was a computer science approach with emphasis on what is important to practitioners of that field, such as computing speed, accuracy of the computation, and size of the computing element. The physical setup of the experiment was not a major factor. Once a working model was determined, the simulation was ready to begin.

2.3 The Parameters/Variables

When light of intensity I hits a thin film of BR, one of two things can occur: it can be absorbed by a molecule in the bR state and switch to the M state, or it can be absorbed by a molecule in the M state and switch to the bR state. Both can happen at the same time. This might seem impossible, but a look at the absorption spectra of BR (Figure 1.3) shows how this can happen. At the wavelength λ = 412nm the M and bR absorption spectra overlap each other. This indicates that some of the molecules can switch from $M \Rightarrow bR$ as expected, but a transition from $bR \Rightarrow M$ is also possible. The process is called forward photoreaction for the former case and back photoreaction for the latter. However with λ = 570nm or higher, the photoreaction for $M \Rightarrow bR$ is insignificant and can be neglected.

The total concentration of BR (concentration is indicated by brackets, e.g. [BR]) is constant because the molecules can only be in either the M or bR state.

This assumption can be made because in the photo-cycle of BR the transition from $M \Rightarrow bR$ is photon driven and, even though the $bR \Rightarrow M$ transition is not totally a photon process, bR relaxes to the M state in pico-seconds after it absorbs a photon. Therefore, it is either in one state or the other. This assumption yields a simple equilibrium equation:

$$[BRo] = [bR] + [M]$$

Where [BRo] is the total concentration of BR in the thin film.

It is possible to come up with a new concentration of bR after it absorbs photons at some wavelength by its forward and back photoreactions. The change in [bR] will be due to the forward photoreaction from $bR \Rightarrow M$, the back photoreaction $M \Rightarrow bR$, and the M decay rate constant K_m. K_m is related to the M state life span τ_M as $K_m = 1/\tau_M$. It is necessary to add a M decay rate constant since, as seen in Figure 1.2, the M state can thermally relax to the bR state. This reaction must be considered because during the time of light exposure some of the molecules will relax from the M state to the bR state. If the M state had an infinite life span then the model would be a pure photoreaction simulation model.

The photoreactions are nothing more than rate $\times$ concentration. For the $bR \Rightarrow M$ conversion, the rate constant $K^{bR \Rightarrow M}$ is multiplied by the concentration of bR, and for the $M \Rightarrow bR$ shift the rate constant $K^{M \Rightarrow bR}$ is multiplied by the concentration of M. The rate constants are, for a given wavelength, light intensity I, quantum yields and molar extinction coefficients, the rate of change from one state to the next. Quantum yield ($\Phi_{bR\Rightarrow M}$ and $\Phi_{M\Rightarrow bR}$) is the probability that a molecule in one state will make the transition to the other state after it absorbs a photon [16]. The molar extinction coefficients ($\epsilon_M(\lambda)$ and $\epsilon_{bR}(\lambda)$) are proportionality constant and differ for each wavelength. Norbert Hampp defines the given rate constants for BR as [15]:

$$K_i^{bR\Rightarrow M} = \frac{2.3026\Phi_{bR\Rightarrow M}\epsilon_{bR}(\lambda_i)\lambda_i I_{oi}}{N_a hc}$$

$$K_i^{M\Rightarrow bR} = \frac{2.3026\Phi_{M\Rightarrow bR}\epsilon_{M}(\lambda_i)\lambda_i I_{oi}}{N_a hc}$$

Where N_a is Avogadro's number, h is Plank's constant, c is the speed of light, I_{oi} is the intensity of the i^{th} wavelength laser beam and λ_i is the wavelength of the i^{th} laser beam. Hampp also provides a differential equation describing the total rate of change of [bR] with respect to time:

$$d[bR]/dt = \sum_{i=1}^{\text{allwavelengths}} -[bR]K_i^{bR\Rightarrow M} + [M]K_i^{M\Rightarrow bR} + [M]K_m \tag{2.1}$$

Dissecting this equation shows a good view of what happens when light is absorbed by BR. [bR]$K^{bR\Rightarrow M}$ gives the change in bR concentration. This is a negative number because the [bR] is decreasing due to the fact that the molecules are changing from the bR state to the M state. For the M state part of the equation, [M]$K^{M \Rightarrow bR}$ = 0 as long as the bR and M absorption spectra do not overlap appreciably at that wavelength. K_m is positive because it adds to the concentration of bR.

The rate of change for [M] is a similar equation except the signs are reversed.

$$d[M]/dt = \sum_{i=1}^{\text{allwavelengths}} [bR]K_i^{bR \Rightarrow M} - [M]K_i^{M \Rightarrow bR} - [M]K_m \tag{2.2}$$

Now [bR]$K^{bR \Rightarrow M}$ is a positive number because the rate change is from bR to M. Therefore, the M concentration is increasing so the M to bR rate is now negative because the switch is to bR not to M. K_m is also negative to show the decay from the M state to the bR state.

Equations (2.1) and (2.2) are linear differential equations that give a non-linear solution with respect to time. Because of what is happening to a film of BR, it is clear why the solution is nonlinear with regard to time. A beam of light hitting the surface of the film will change molecules from one state to the the other. Given enough time, all the molecules will switch to the other state, which is saturation. When saturation is reached, the light no longer has any effect on the sample. Figure 2.1 shows how the concentration changes, until it reaches saturation over a period of time.

The formulas are linear but our process is a nonlinear process. So time, in-tensity, thickness and concentration are important parameters in the project. By

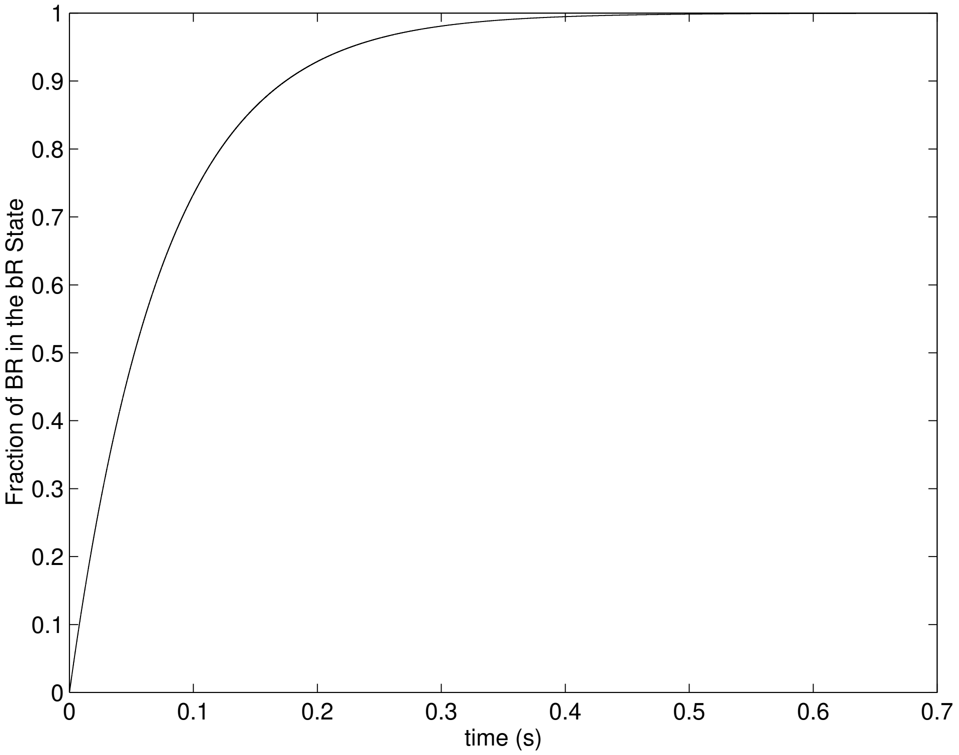

Figure 2.1: Saturation of BR

manipulating these, the simulation can stay within the linear region of the photoreaction process.

2.3.1 Time, Intensity, Thickness and Concentration

When light hits the surface of a BR film, it is either reflected, absorbed or transmitted. The reflected amount is assumed to be so insignificant that it can be neglected. The amount of light transmitted depends on the thickness of the film d, concentration of the film, intensity of the initial light I_o, and the duration of the exposure time t. By using the Beer-Lambert law, Robert R. Birge, a pioneer in the study of BR, derived an equation to calculate the light transmitted through a thin film of BR:

$$I_n = I_{o(n-1)} \exp(-2.3026 d_n \{\epsilon^M(\lambda)[bR] + \{\epsilon^{bR}(\lambda) - \epsilon^M(\lambda)\} \frac{[bR]}{BRo}^n [BRo]\}) \quad (2.3)$$

This calculation is determined recursively. The film is divided into n slices. Each iteration through the film depends on the previous slice's concentration of bR (which is represented by $[bR]^n$ in equation 2.3), [M] and light intensity. The equation mimics the effect of what happens in a sample when it is hit by some light. More molecules closer to the surface have switched to the other state than at the bottom of the sample because light intensity decreases with thickness, so fewer molecules are converted (see Figure 2.2). Increasing the light intensity will cause an increase in the conversion rate which would result in a faster saturation time for the film.

2.4 The Model Computational System

In the model, the following assumptions are made:

- reflection is negligible
- the amount of time spent in each layer is the same
- the BR in the thin film is oriented

There are formulas to solve for the change in [bR] and [M] and the change in intensity through the thin film. Combining these together, we derive a model of light being absorbed by a thin film of BR.

2.4.1 Addition

The template for the addition experiment is shown in Figure 2.3. First, the X thin sample is written into by light of intensity I_x and wavelength of ω_1, likewise the Y sample is written into by light of intensity I_y with a wavelength of ω_1. Then, the X and Y thin samples are read by a light of intensity I_r with a wavelength of ω_2. The time for writing and reading of the samples are two distinct time

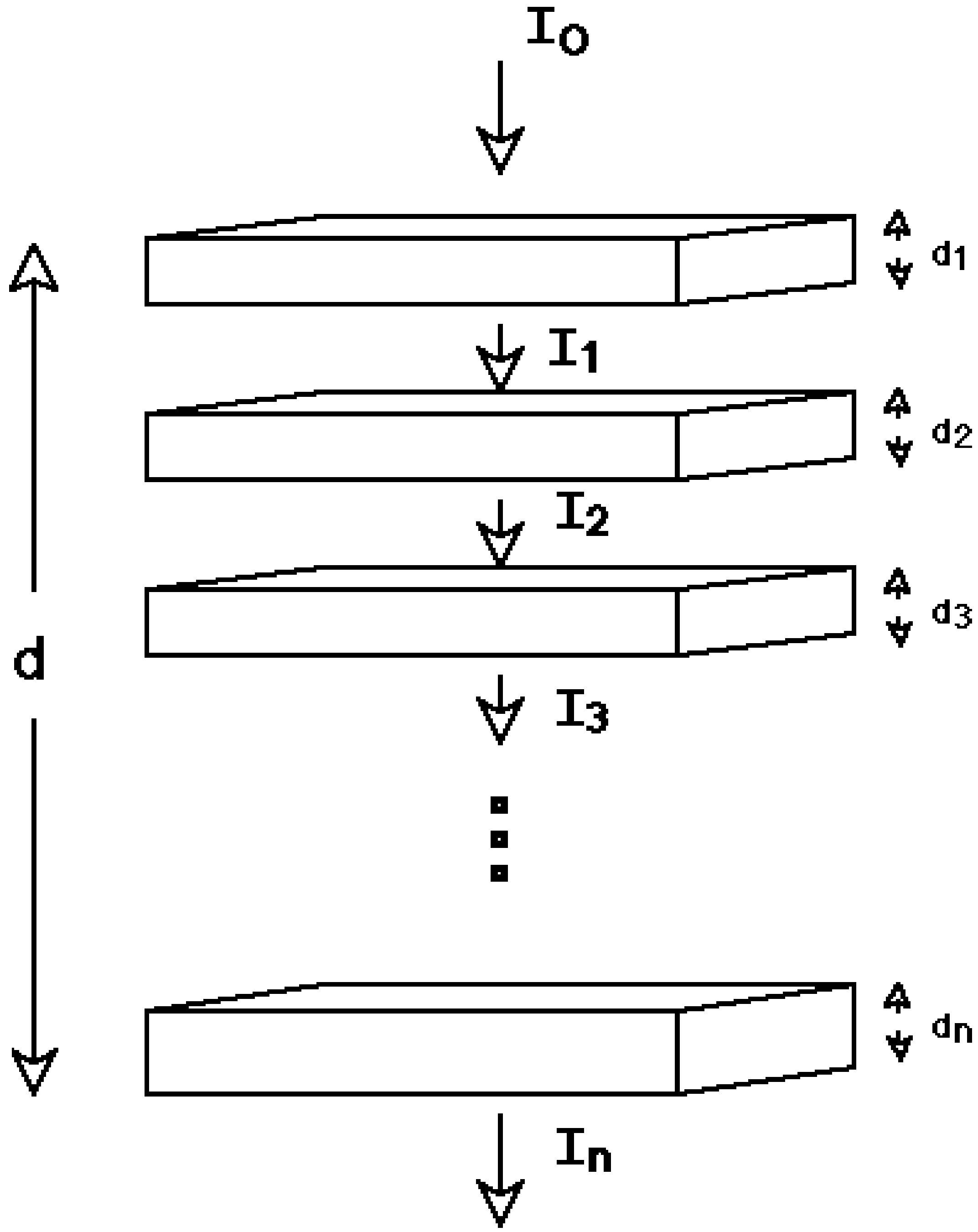

Figure 2.2: Light permeating through a thin sheet of BR layer by layer. As d_n increases I_n decreases.

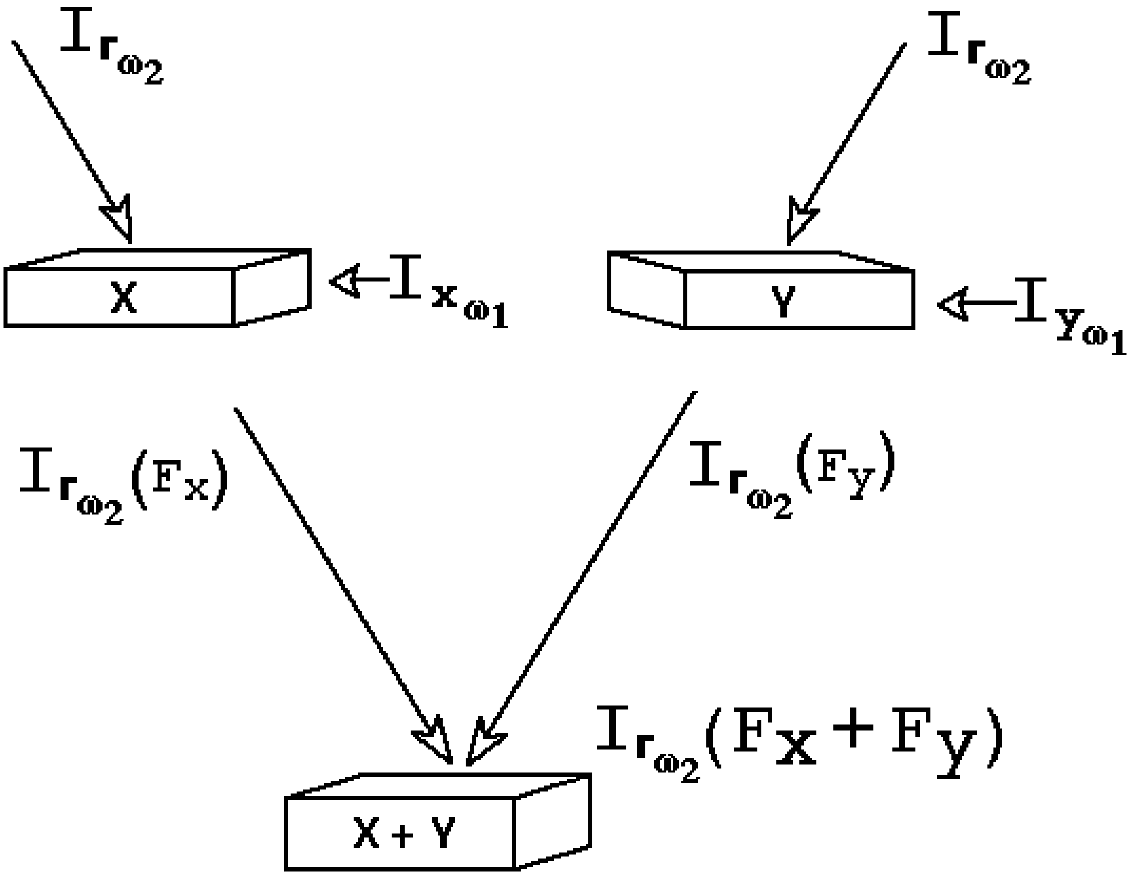

Figure 2.3: The template for the addition of two thin film of BR

periods, and they are not necessarily the same throughout the experiment. The read and write intensities are constant through the run of the experiments. The initial concentration of the BR in the samples depends on the write wavelength. For example, if the write wavelength is 413nm then the initial concentration of BR molecules will almost all be in the M state. Likewise, if the write wavelength is 568nm then the BR molecules will be in the bR state. However, the same initial concentration for the X + Y thin sample depends on the read wavelength.

The write intensities of light will switch some amount of molecules to one state in the X and Y samples. Then the read intensities of light will also switch some amount of molecules from one state to the other, with some of the light transmitted through the sample. At this point in the computation there is a transformation of medium, meaning that the light transmitted is a function of X and Y that was originally in the sample. When both beams hit the third film, their intensities will change the state of the film giving the addition of X and Y. In the above explanation, I hesitate to use numbers because at this point in the paper it is not possible to say that if 10% of X and Y are converted to bR then the addition is 20% of bR. Once the behavior is characterized, the addition experiment can match the conversion to some range of numbers. An exact match is not expected, but the goal is to be within a 10% error range because this is the approximate precision of neural computation.

2.5 Characterization

To get the best parameters for this experiment, characteristic tests were run on the thin film to see what kind of reaction would result. Characteristic tests include varying factors of depth, wavelength, and read and exposure time. One such test was to see the rate of change per slice in the thin film at different intensities per wavelength. Figure 2.4 shows how the depth of the thin film affects the BR concentration. Also, the circumstances under which saturation was achieved for reading and writing in the sample were examined. These initial experiments gave insight on what parameters would work best in the model.

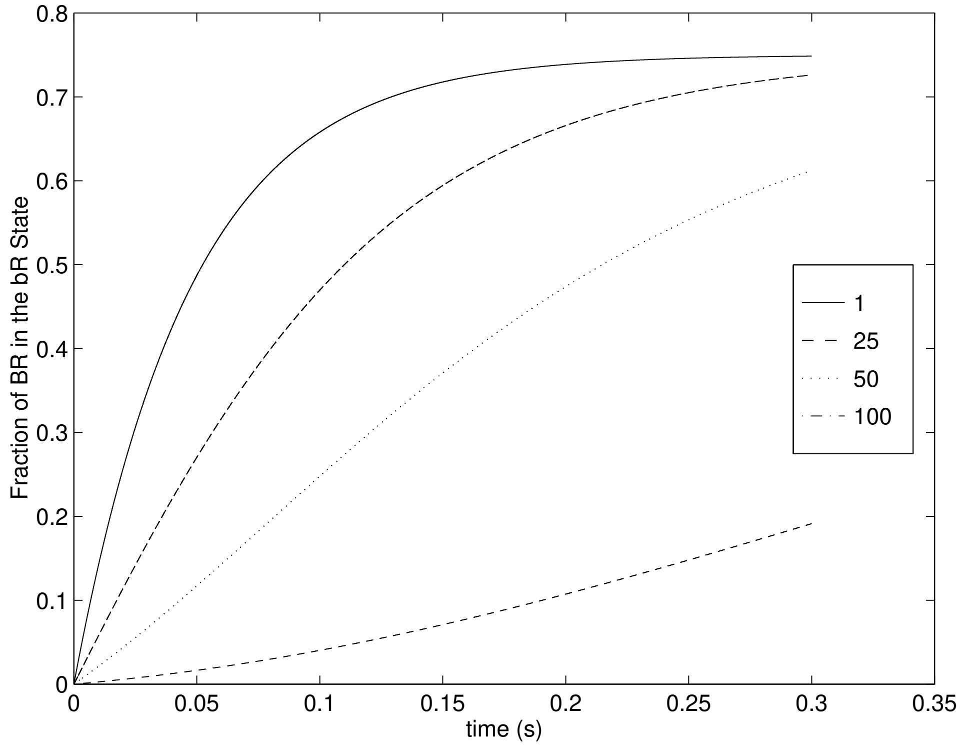

Figure 2.4: The graph shows the concentration of bR in the BR sample per layer.

Chapter 3

Interpretation of the Results

3.1 Addition Experiments

Since there are two different wavelengths, there are four possible ways to perform the addition experiment described in Chapter two. The first two ways are to write with the 413nm wavelength and then read with the 568nm or write with the 568nm wavelength and then read with the 413nm wavelength. The two other scenarios are to write with a wavelength of 568nm and read with 568nm wavelength or write with a wavelength of 413nm and read with the 413nm wavelength. All four situations were simulated in the computational model with the same write and read times and read intensities. The experiments could be separated into two basic types, same wavelength experiments and different wavelength experiments.

3.1.1 Scheme One

The setup in Figure 3.1 shows the experiment of writing with a wavelength of 413nm and reading with a wavelength of 568nm. Initially the BR in samples X and Y is all in the M state and the BR in the sample X+Y is all in the bR state. X and Y are written into by shining a light of wavelength 413nm on their surface, converting some of the M to the bR state. The amount of conversion

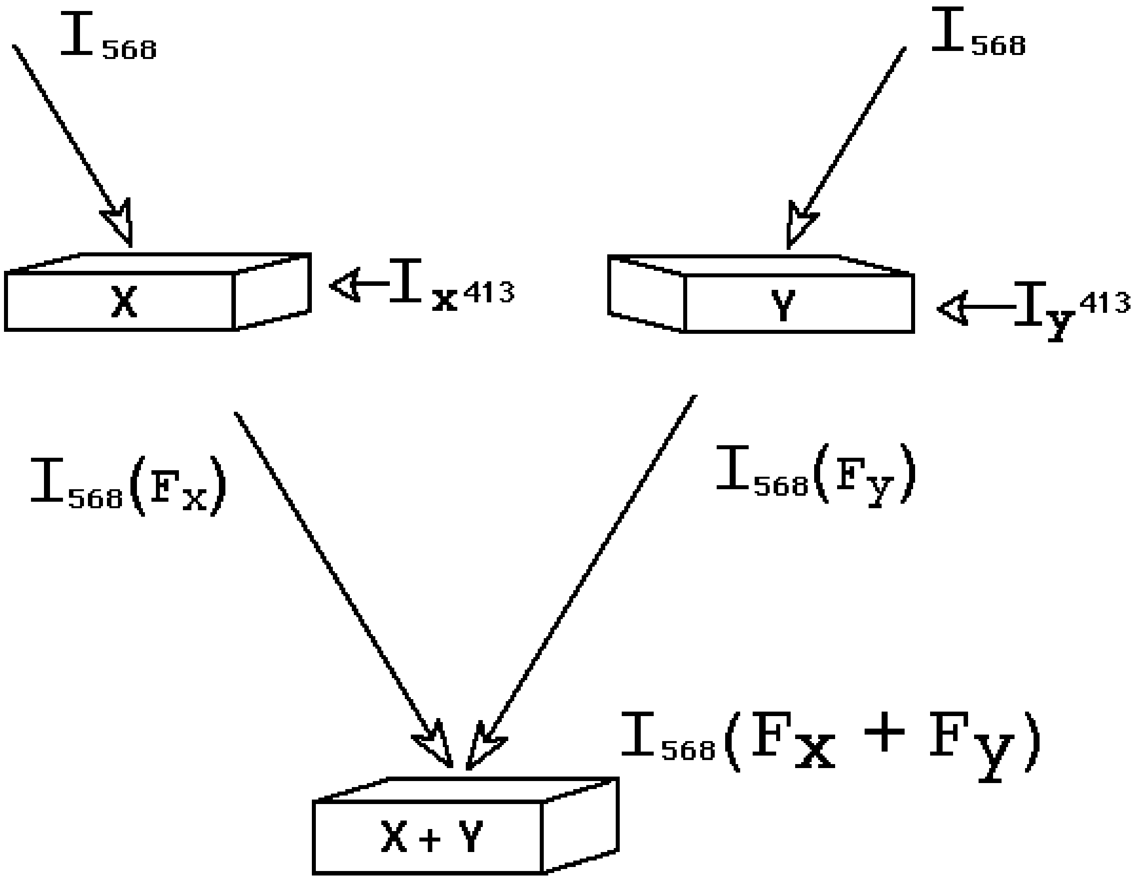

Figure 3.1: Writing with a wavelength of 413nm and reading with a wavelength of 568nm.

depends on intensity and time of exposure on the film. Then a light of 568nm wavelength is shone through X and another light of the same wavelength is shone through Y. The 568nm wavelength will be absorbed by the bR in the sample and transmission depends on the percentage of molecules in the M state. The transmission coming from X and Y will be absorbed, switching the BR in the X + Y thin film from its initial state of bR to the M state. The X + Y thin sample now has the correct amount of BR in the bR state.

3.1.2 Scheme Two

This experiment is the reverse of the first read and write into X and Y, where initially the BR are all in the bR state, with light of 568nm wavelength. Then a light of 413nm wavelength is shone through X and Y. The transmission coming from X and Y will be absorbed, switching the BR in the X + Y thin film from its initial state of M to the bR state. Therefore Figure 3.2 is the same as Figure 3.1 but with the read and write wavelengths reversed. Here, what is taking place is writing in the thin film with different write intensities of the 568nm wavelength and reading out with a constant read intensity of light at 413nm wavelength.

3.1.3 Scheme Three

This addition has a different setup. The writing light and reading light are the same. This makes the initial state of BR the same for the input, sample X and

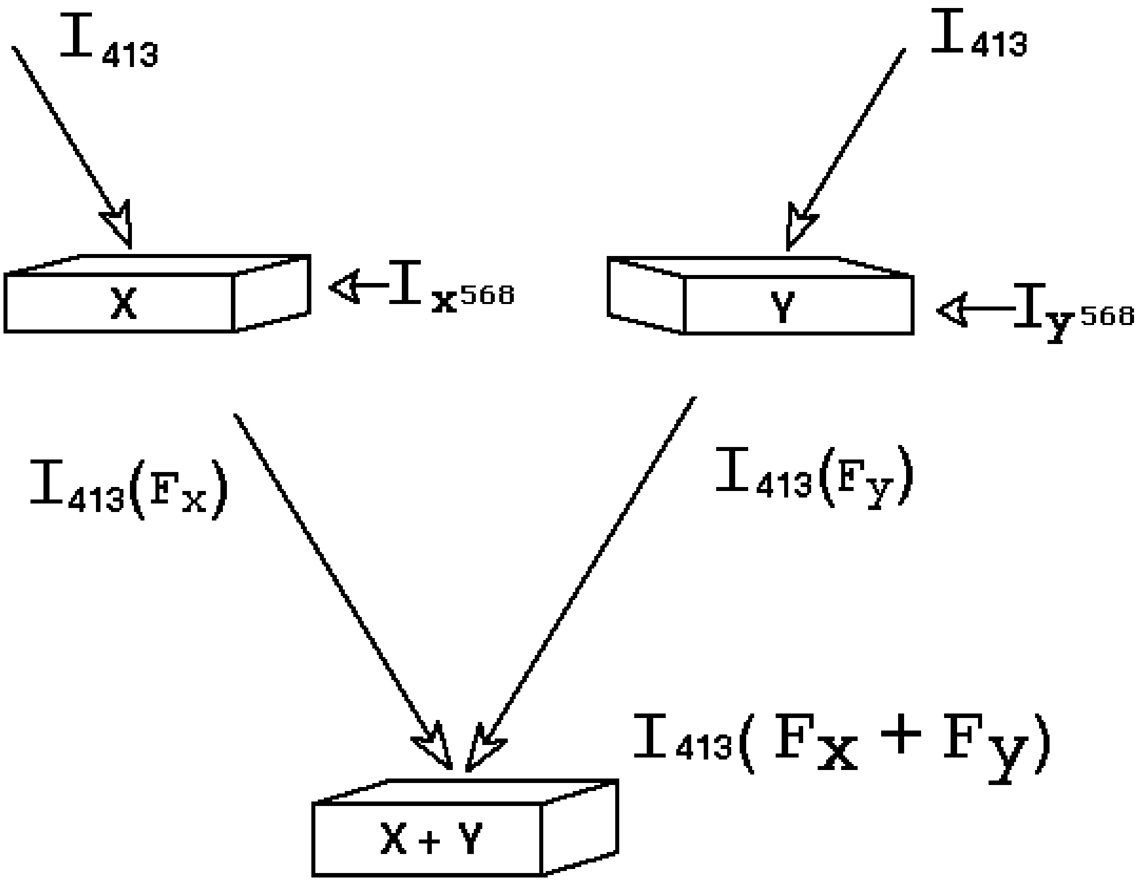

Figure 3.2: Writing with a wavelength of 568nm and reading with a wavelength of 413nm.

sample Y, and output, sample X + Y. In this case they will all be in the bR state. A light of 568nm is shone on the thin film X and Y, and then another light of the 568nm wavelength is shown through X and Y again. The transmission of this light is absorbed by the X + Y film. This converts the initial BR in the bR state in the film to the M state. Figure 3.3 shows the scenario clearly. The write

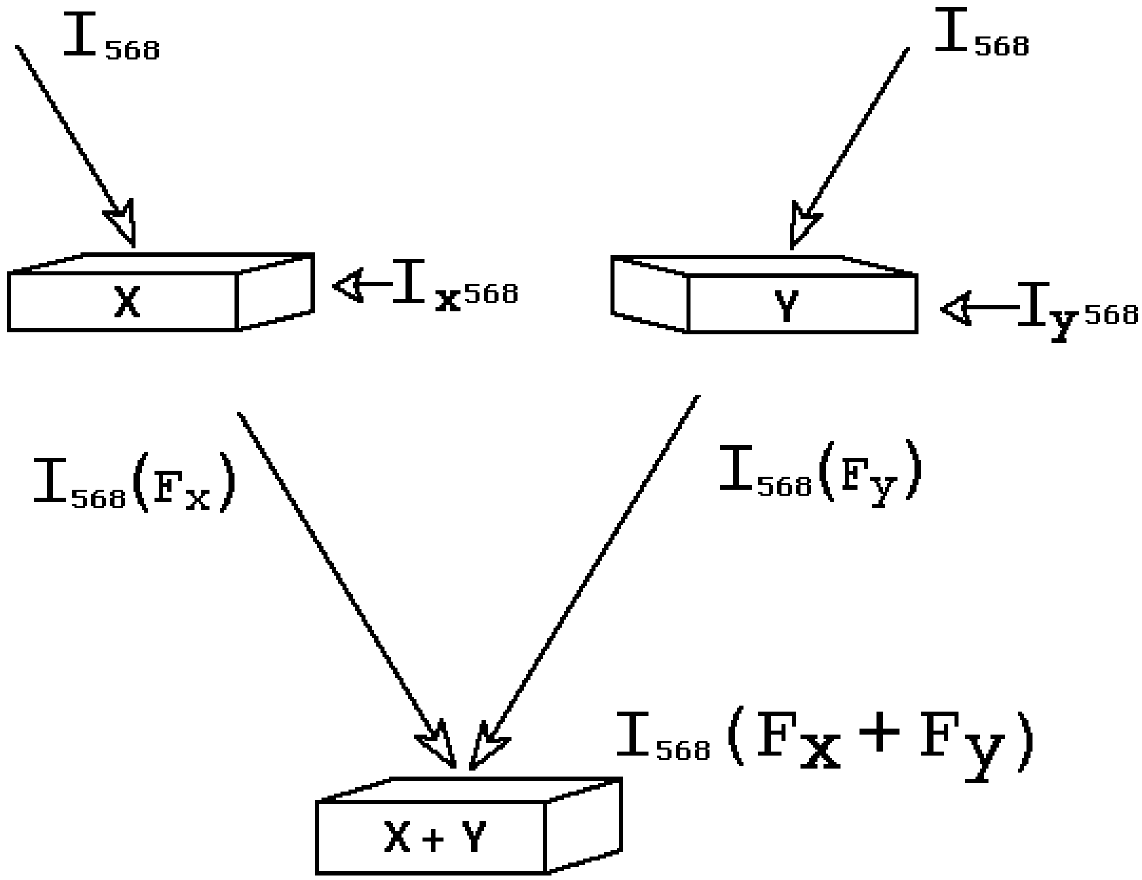

Figure 3.3: Writing with a wavelength of 568nm and reading with a wavelength of 568nm.

light converts some amount of BR from bR state to the M state for both X and Y. Then the read light is absorbed by the rest of the BR in bR state, converting all (or almost all) into the M state but the amount of the BR in the M state will be a function of light that it shines through or the transmission.

3.1.4 Scheme Four

This scheme (Figure 3.4) is the same as Scheme Three but it uses light of 413nm instead of 568nm. The initial state of BR in the input and output sample will be in the M state for this case. A light of 413nm is shone on the sample X and Y, and then another light of the 568nm wavelength is shown through X and Y again. The transmission of this light is absorbed by the X + Y film. This converts the initial BR in the M state in the film to the bR state.

3.2 Results

During the experiment, data were collected and separated for the writing into the thin sample and the reading of the thin sample. Once the read and write times are initially set up they are kept constant throughout each complete run.

Examining the results of Scheme Three, Figure 3.5 shows the write part of the experiment with a write time of 0.03ms and an intensity from 0 to a 100mW. In Figure 3.5, it is obvious that the top layers of the sample have a greater concentration of molecules in the M state than the bR state because less light of 568nm

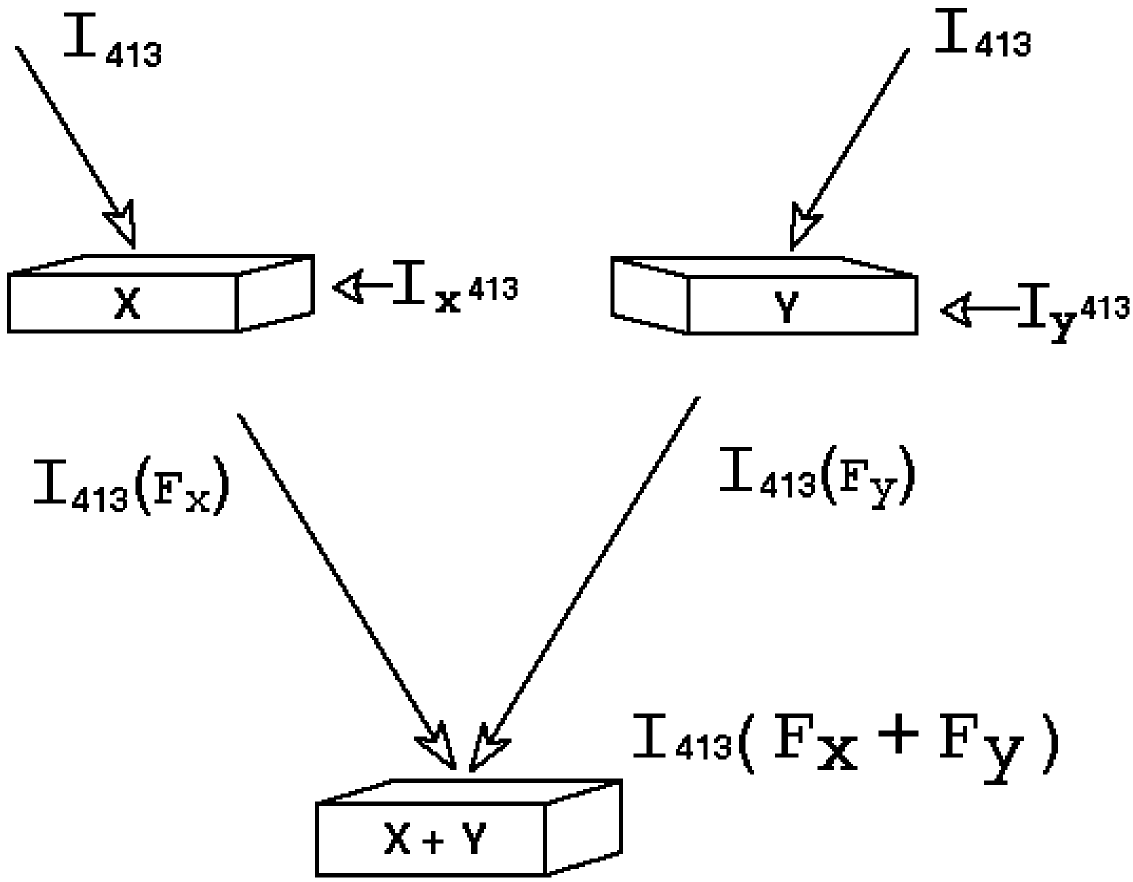

Figure 3.4: Writing with a wavelength of 413nm and reading with a wavelength of 413nm.

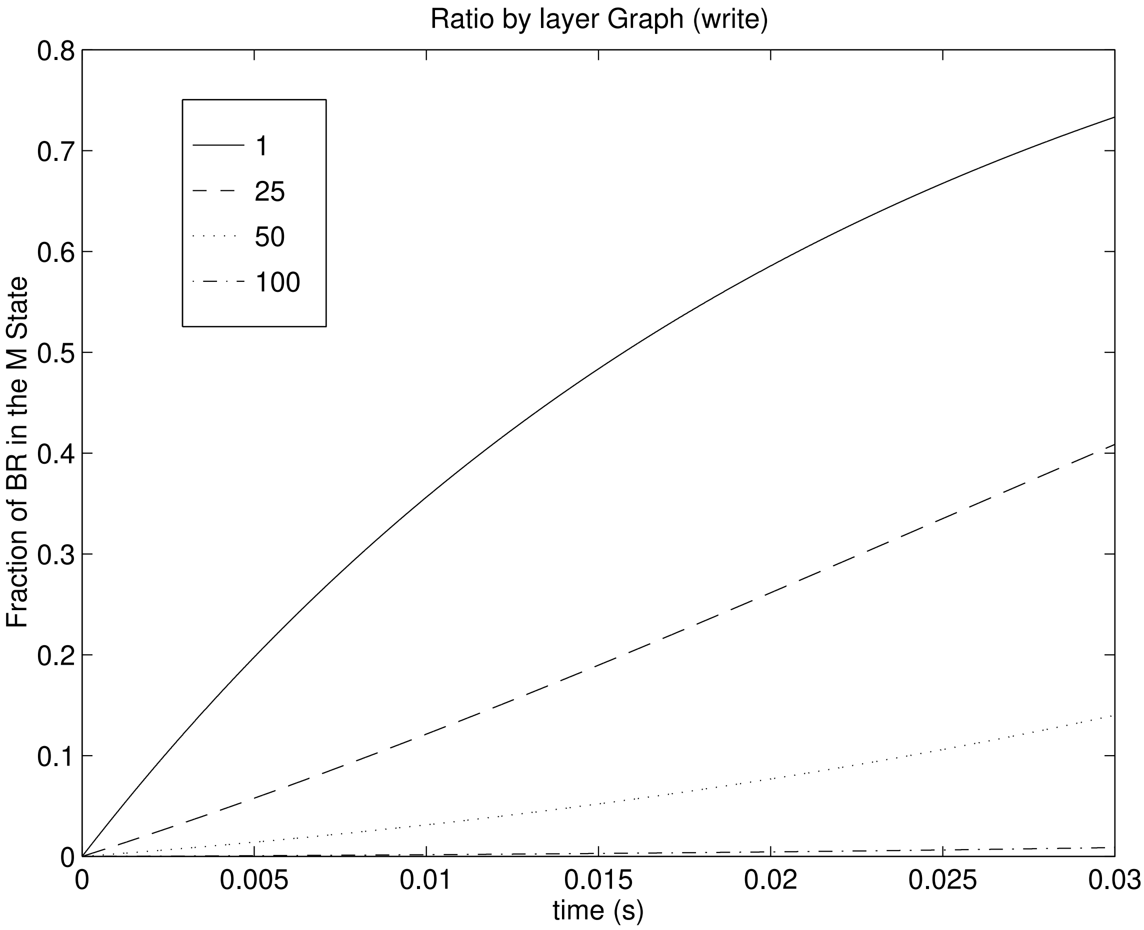

Figure 3.5: The thin sample is broken up into a 100 slice and the graph shows the concentration of M in layer 1, 25, 50 and 100 during the write phase.

is reaching the lower layers of the sample, resulting in less conversion of molecules in the bottom region. The average fraction of BR in the M state in the sample is shown in Figure 3.6.

In the read phase of the Scheme Three experiment, concentration per layer is rising because the read phase begins and continues where the write phase finishes. This is the fundamental problem with the same wavelength read and write setup. The write concentration is destroyed on the read phase, and the initial concentration cannot be retrieved again. Figure 3.7 shows the fraction of BR in the M state per layer of the read portion, and Figure 3.8 displays the average fraction

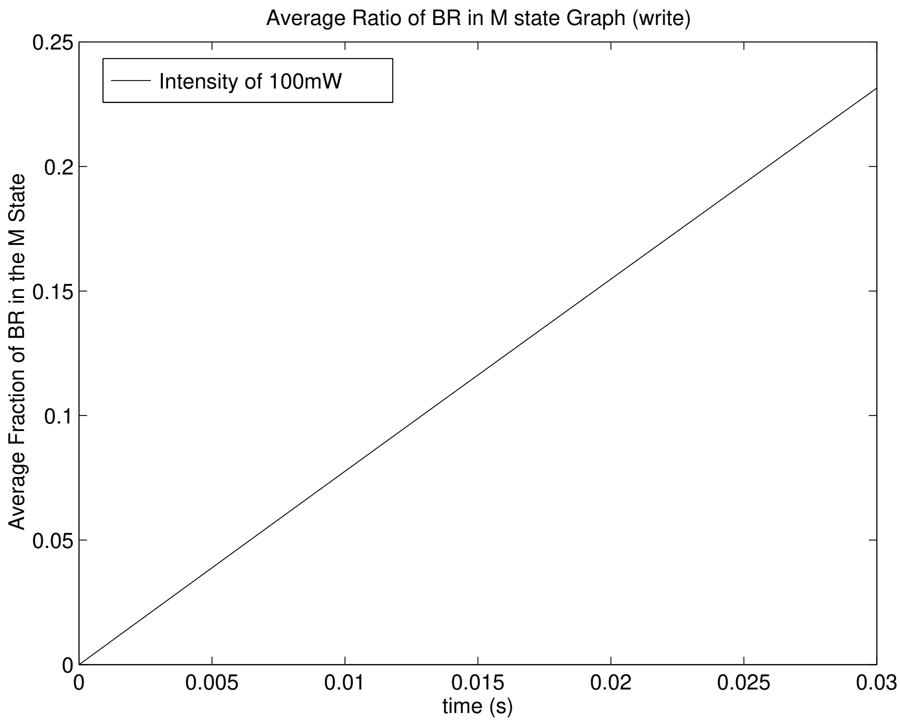

Figure 3.6: The average fraction of BR in the M state during write phase.

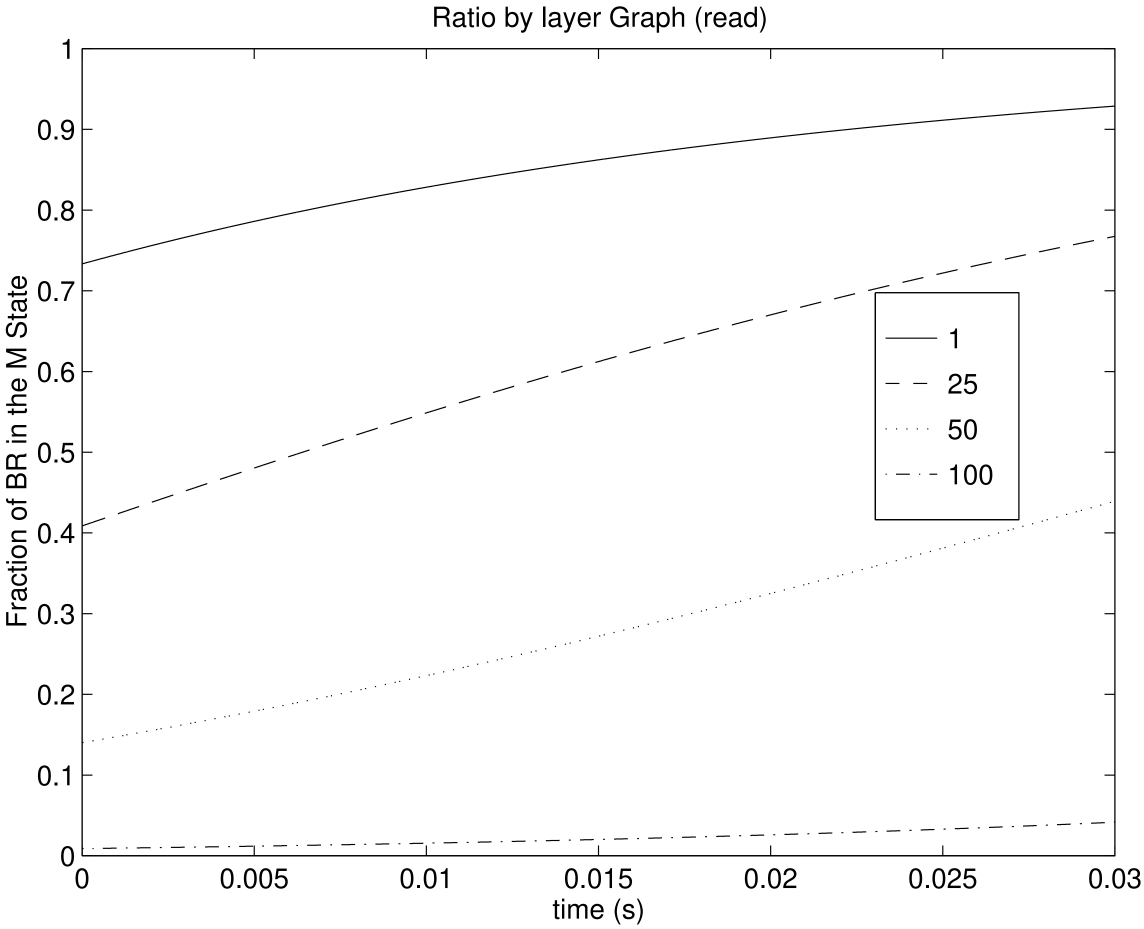

Figure 3.7: The thin sample is broken up into a 100 slice and the graph shows the concentration of M in layer 1, 25, 50 and 100 during the read phase.

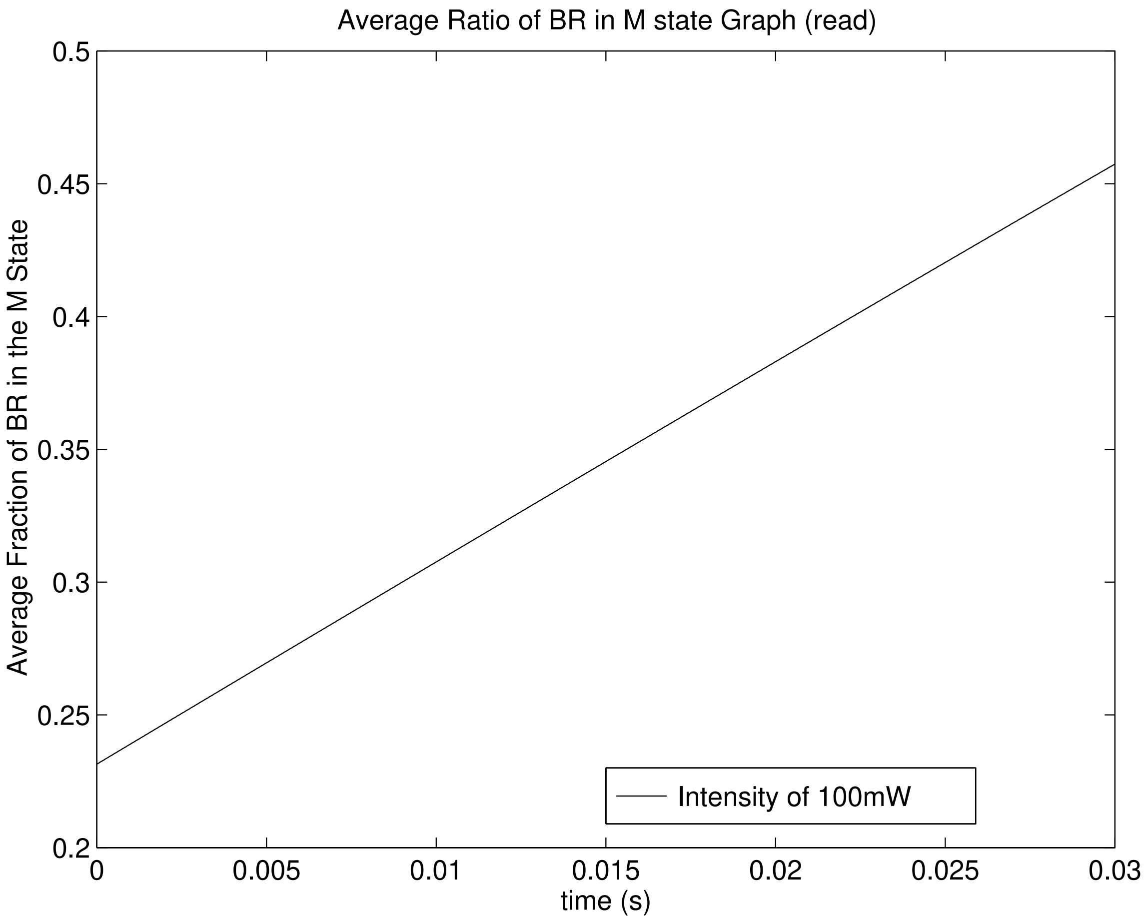

Figure 3.8: The average fraction of BR in the M state during read phase.

of BR in the M state of the thin sample. Notice that the read phase does not start at 0 for the average, but begins where the write phase left off in Figure 3.8. Finally, Figure 3.9 shows the transmitted light through the thin sample. The transmitted light is relatively low at this point because more light is being absorbed than being passed through, due to the fact that there is more BR in the bR state when the sample was read.

In Scheme Four, the light was incident upon the sample with a write and read time of 0.03ms and was exposed to a light intensity of 400mW and 100mW. In Figure 3.10, the fraction of bR per layer at an intensity of 100mW is shown.

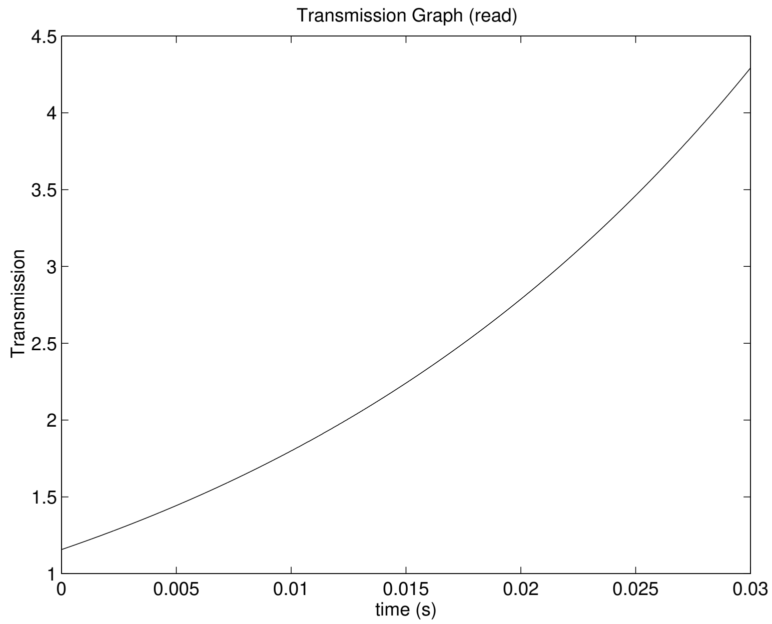

Figure 3.9: The average transmission state during read phase.

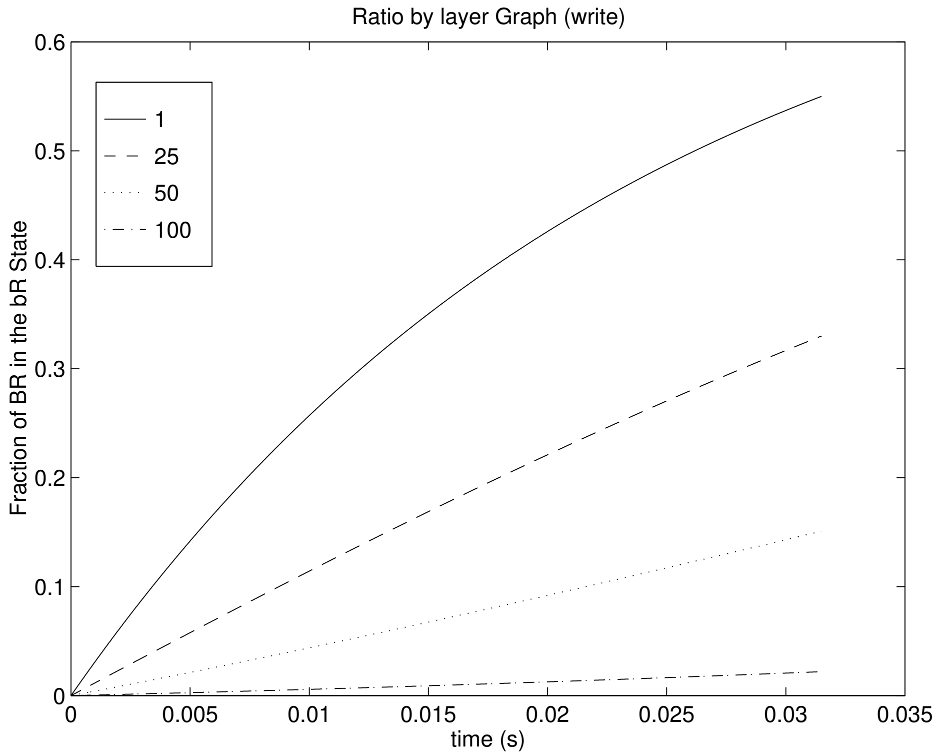

Figure 3.10: The thin sample is broken up into a 100 slice and the graph shows the concentration of bR in layer 1, 25, 50 and 100 during the write phase.

The top layer had more molecules switch from the M state to the bR state than the lower layers (the light is causing molecules to switch from the M to the bR state since the wavelength is 413nm). Figure 3.11 is the average fraction of molecules in the bR state over the write time for an intensity of 100mW. The fraction of bR per layer at an intensity of 400mW is seen in Figure 3.12, and for an intensity of 400mW, Figure 3.13 is the average fraction in the bR state over the write time. In the read part of this experiment, the data that is needed is the transmitted

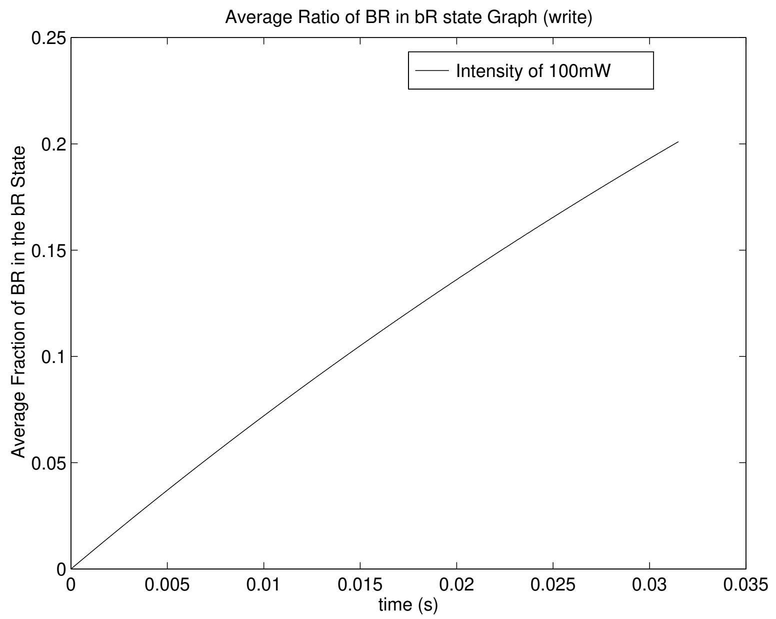

Figure 3.11: The average fraction of BR in the bR state during write phase.

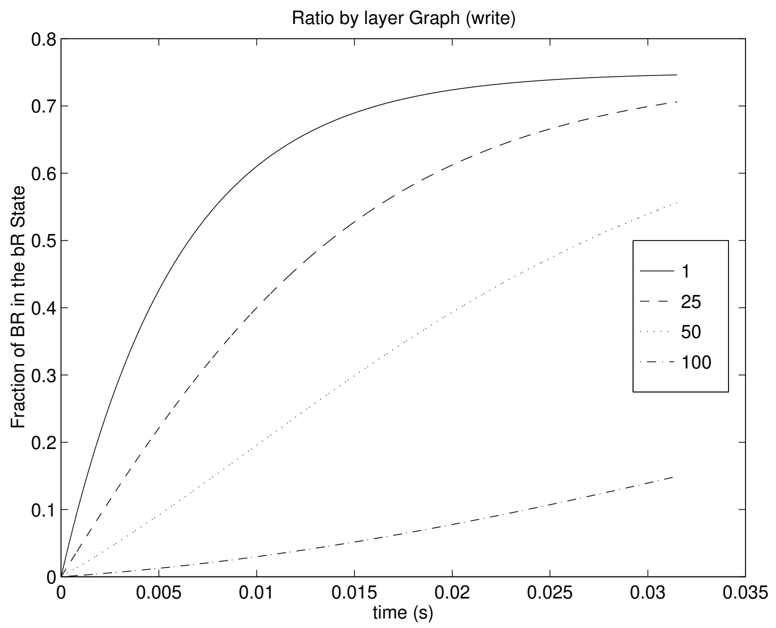

Figure 3.12: The thin sample is broken up into a 100 slice and the graph shows the concentration of bR in layer 1, 25, 50 and 100 during the write phase.

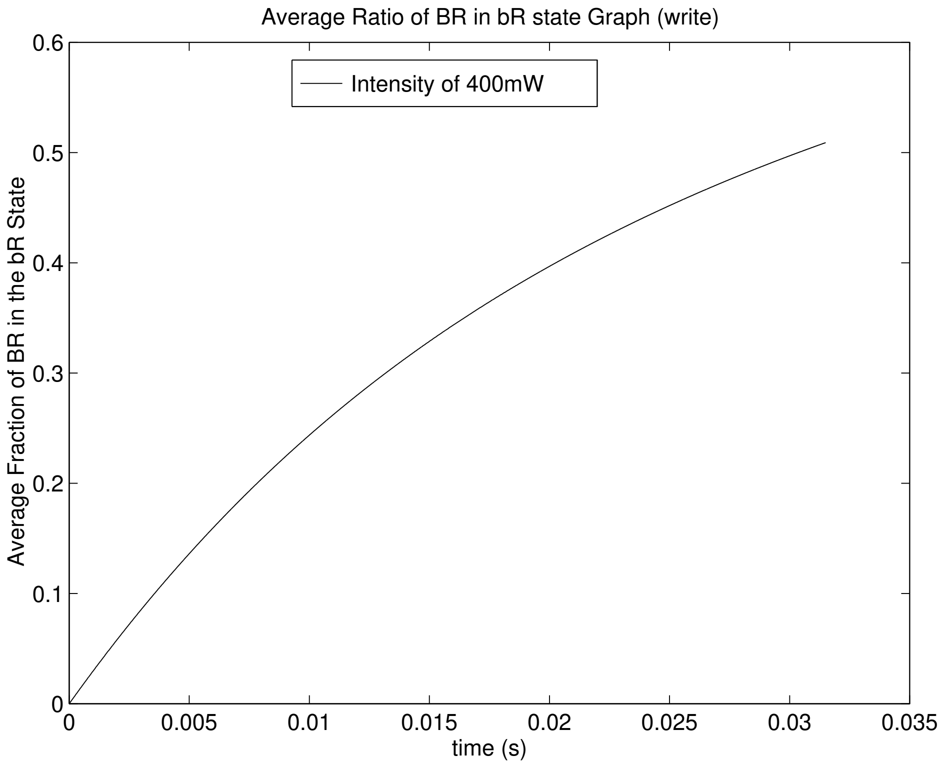

Figure 3.13: The average fraction of BR in the bR state during write phase.

light through the sample. Figure 3.14 shows the transmitted light when the read intensity is 100mW and Figure 3.15 read intensity is 400mW. As expected, more light is transmitted with 400mW intensity then with 100mW.

Scheme One is the setup using two different wavelength for read and write (see Figure 3.1). A wavelength of 413nm is written into the sample which is read with a wavelength of 568nm. This setup can be seen as the combination of the other two same wavelength experiments described in the two paragraphs above. The write phase of Scheme One is the same as the write for Scheme Four and the read phase of Scheme One is the same as the read of Scheme Three. So the setup is

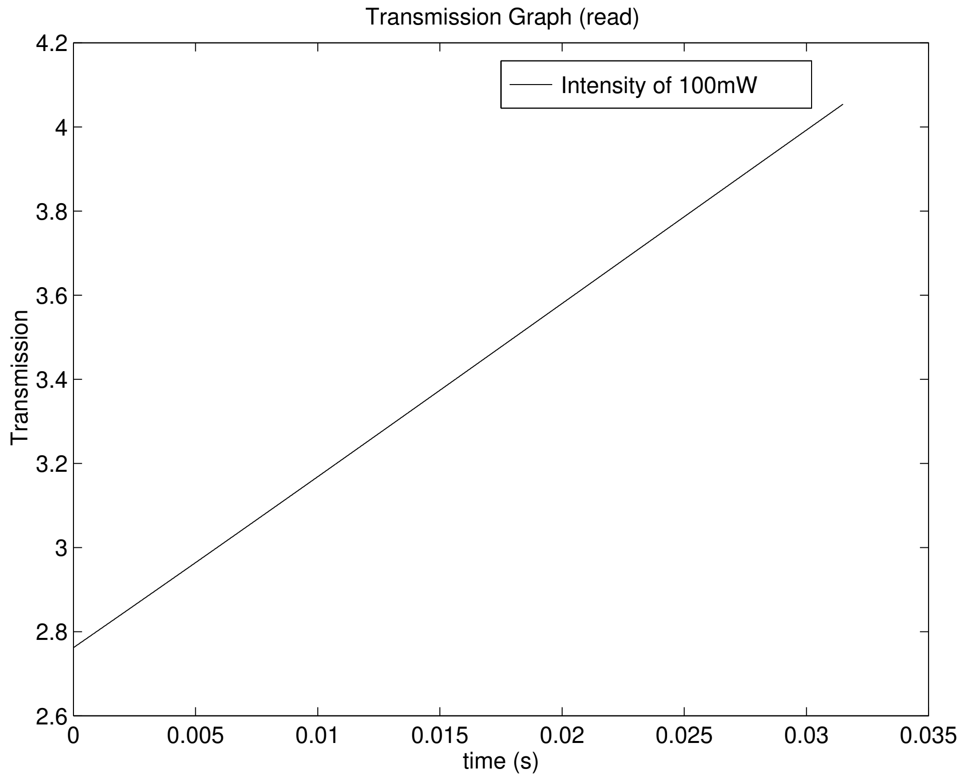

Figure 3.14: Transmission of the sample during reading at 100mW.

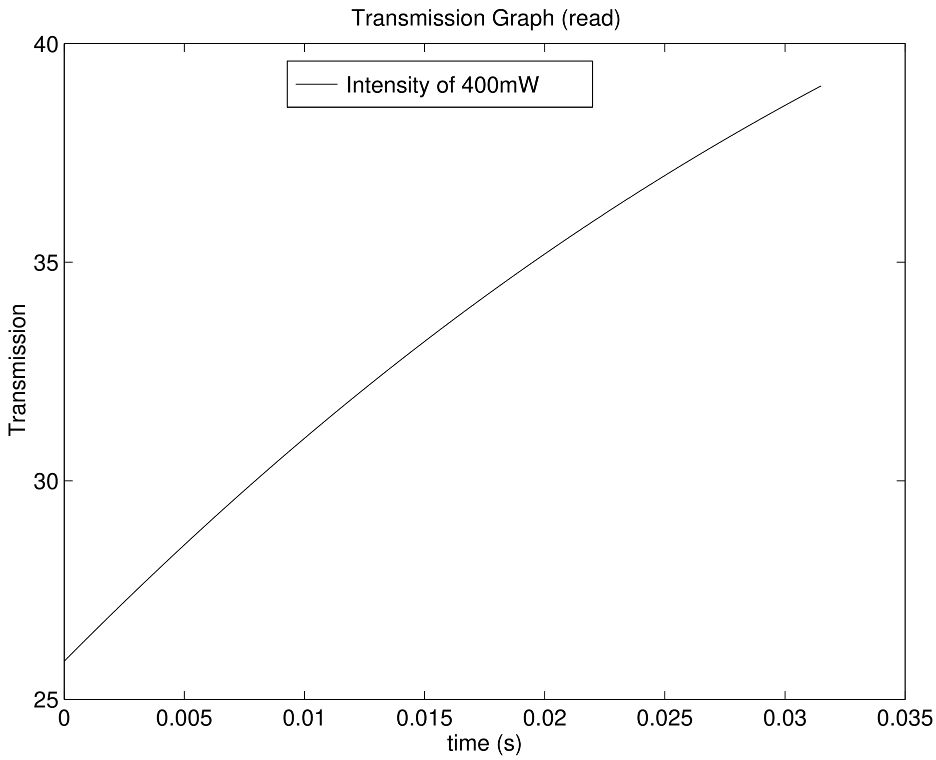

Figure 3.15: Transmission during reading of the sample at 400mW.

not unique, but this experiment emphasizes the crucial difference in the two basic experiments (same and different wavelengths). With the same wavelength experiment the data is corrupted after it is read, but with the different wavelength experiment there are a couple of ways to ensure that the initial writing is preserved by using the second harmonic or double photon method (see [7] and [5]). In this experiment, neither of these methods are used because a subsequent read of the initial X or Y was not needed. If some wavelength (413nm) is written into the sample for time τ_w and then read with a different wavelength (568nm) for time τ_r, it is important to understand what the output transmission will be in this experiment.

For Scheme One, Figure 3.16 shows the input intensity versus the average output transmission for different read and write times and for different read intensities. In Figure 3.16, the write and read time is the same for each run (0.03ms write time and 0.02ms read time), but the read intensity is different. The read intensity ranges from 96 to 150mW and the write and read times were between 0.01ms to 0.07ms. At a write intensity of 0mW, all the BR molecules are in the M state in the samples. Since the write intensity is zero there is no change to the sample, so from the perspective of the read light (568nm), saturation has occurred in the sample (all the molecules are in the M state). Therefore, most of the read light is transmitted though the sample. In Figure 3.17 shows the read input versus the light transmission where the read intensity is the same throughout the

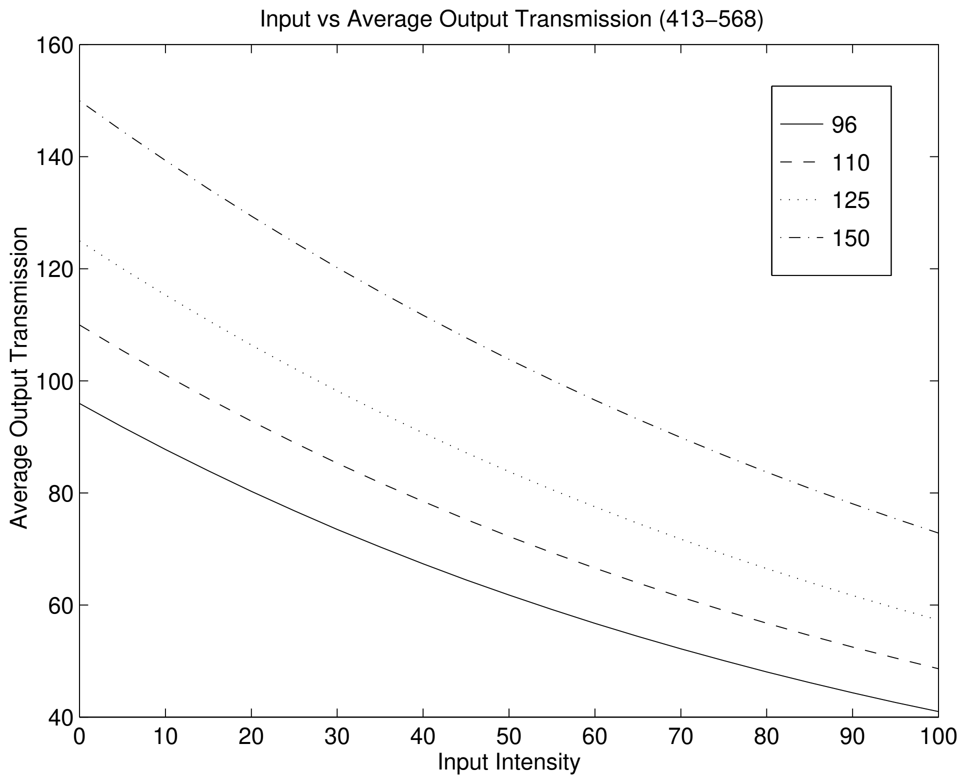

Figure 3.16: The read and write time are the same while the intensity changes.

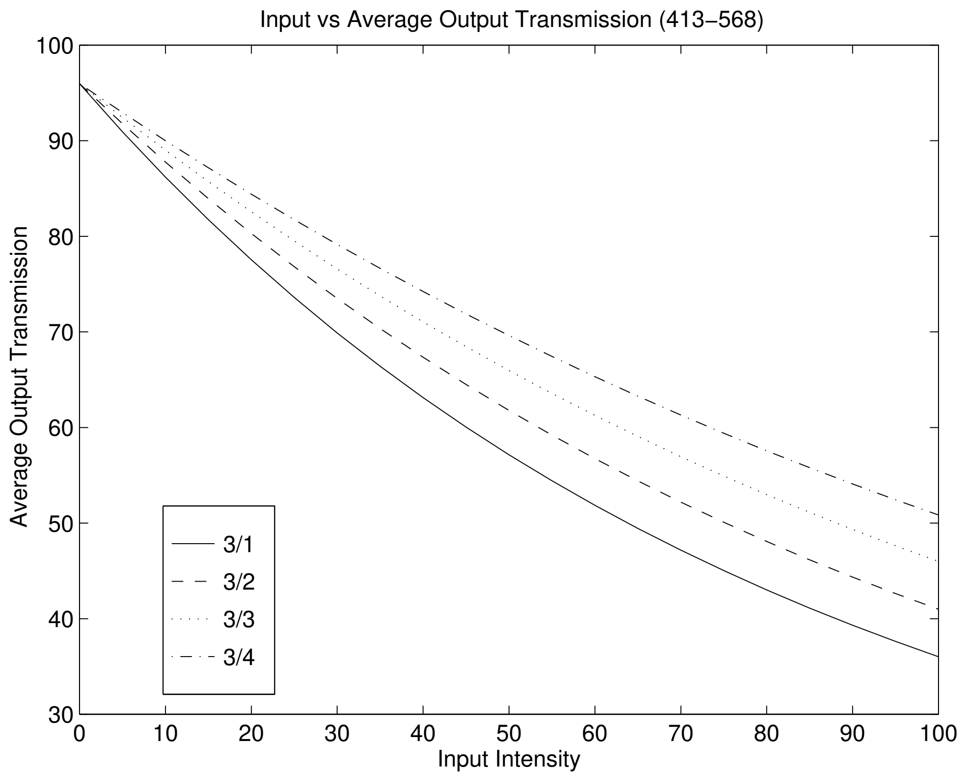

Figure 3.17: The intensity is the same while the read and write time are changing.

experiment and the read and write time was varied. In Figure 3.17 the plots do not have straight lines because the rates of changing for each state are not equal so the result is a slightly curved line.

As shown in Scheme Two, where the experiment writes with a wavelength of 568nm and reads with a wavelength of 413nm, the write and read times and the read intensity vary. The read and write times range from 0.01ms to 0.06ms and the read intensity was from 400mW to 700mW. Figure 3.18 shows the input versus

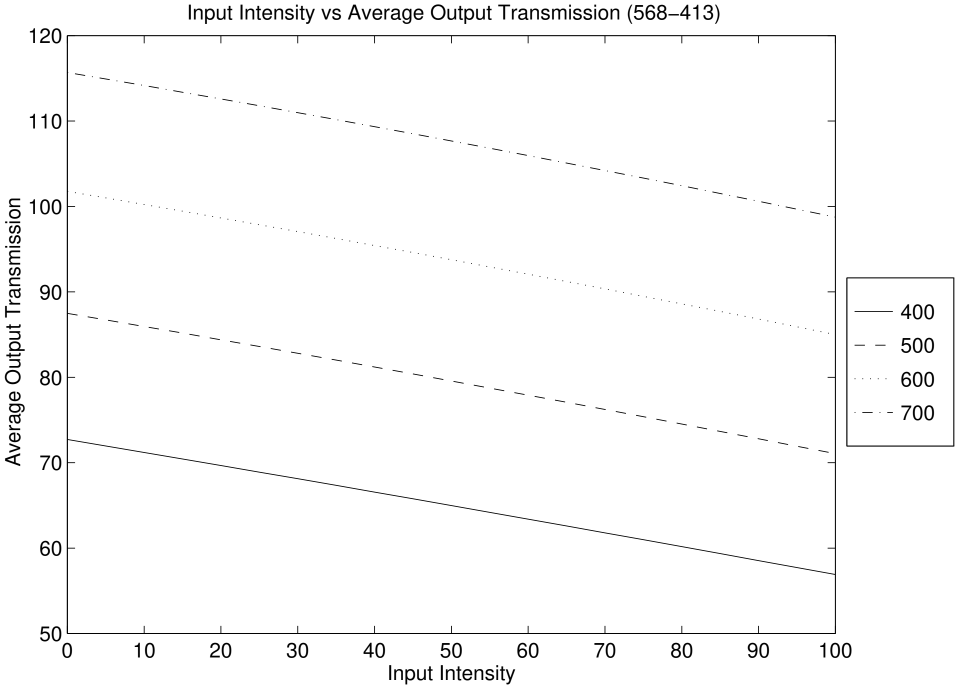

Figure 3.18: The read and write time are the same while the intensity changes.

output for this experiment. The read and write times (0.03ms and 0.02ms) are constant throughout the experiment, while the read intensity varies from 400mW to 700mW. In Figure 3.19, the read and write times vary while the read intensity remains the same at 400mW throughout the experiment. What is noticeable about these graphs is that the output transmissions are not large considering the degree of read intensities, and the lines are fairly straight in Figure 3.18 and 3.19.

3.3 Analysis

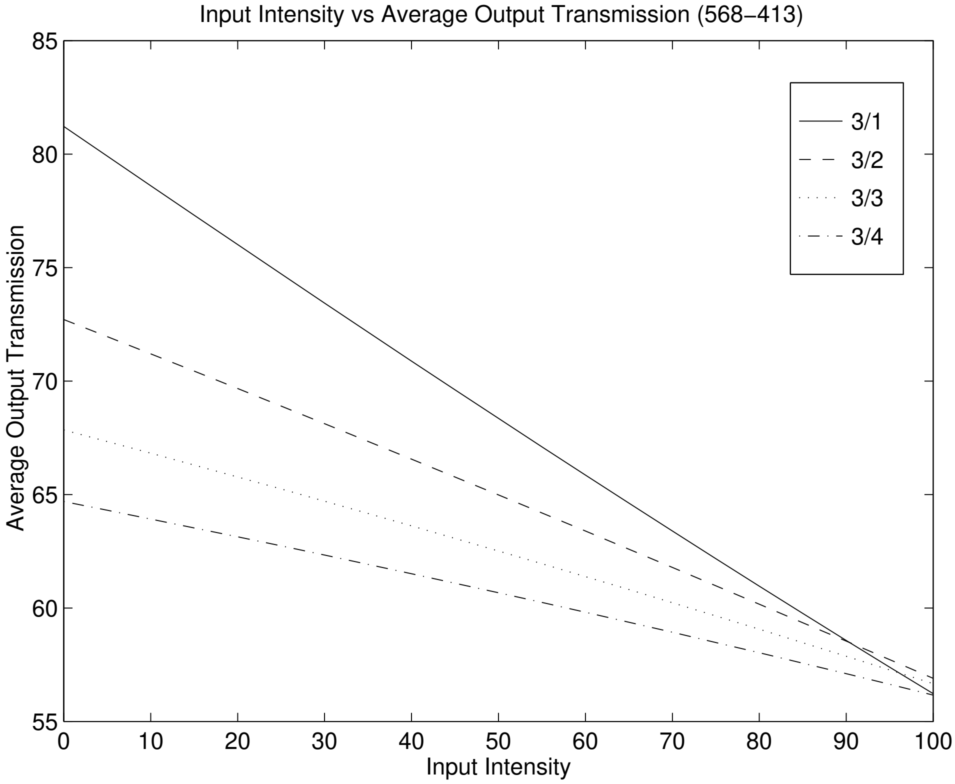

Figure 3.19: The intensity is the same while the read and write time are changing.

3.3.1 The Good, The Bad and The Ugly

The experiments with the same read and write wavelength were not suitable for the needs of these experiments. In the case with the wavelength of 413nm, the transmission during read was only a fourth of the read intensity (See Figure 3.20), meaning more power was needed. The main reason that the same state setups were not used was that the results of the addition would be in the inverse state after the X + Y sample was read. For example suppose a sample is written into with a wavelength of 568nm converting some of the BR in the bR state to the M state. Then, a read is performed at the same wavelength causing additional switching of molecules in the bR state to the M state. The amount of the transmission depends on the concentration of M after the write. This transmission will in turn convert the BR (in the X + Y sample of Figure 3.21) into M state. Now when a read is done to see the answer, it will be the concentration of bR that represents the solution, not the concentration of M in the sample. This is also the same situation for writing and reading with a wavelength of 568nm.

The experiments with the different read and write wavelengths do not give an inverse answer when the solution is read. For example suppose a sample is written into with a wavelength of 413nm converting some of the BR in the M state to the bR state. Then, a read is perform, with a wavelength of 568nm switching molecules from the bR state to the M state. The amount of the transmission

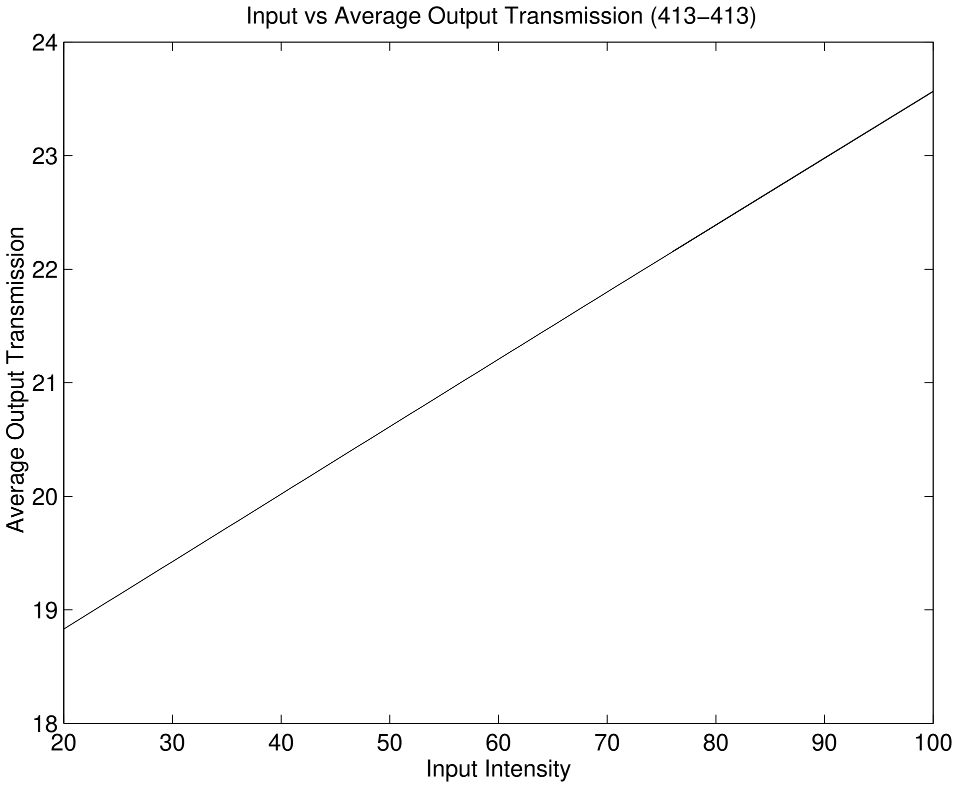

Figure 3.20: The same wavelength setup gets transmission of roughly one fourth the input power.

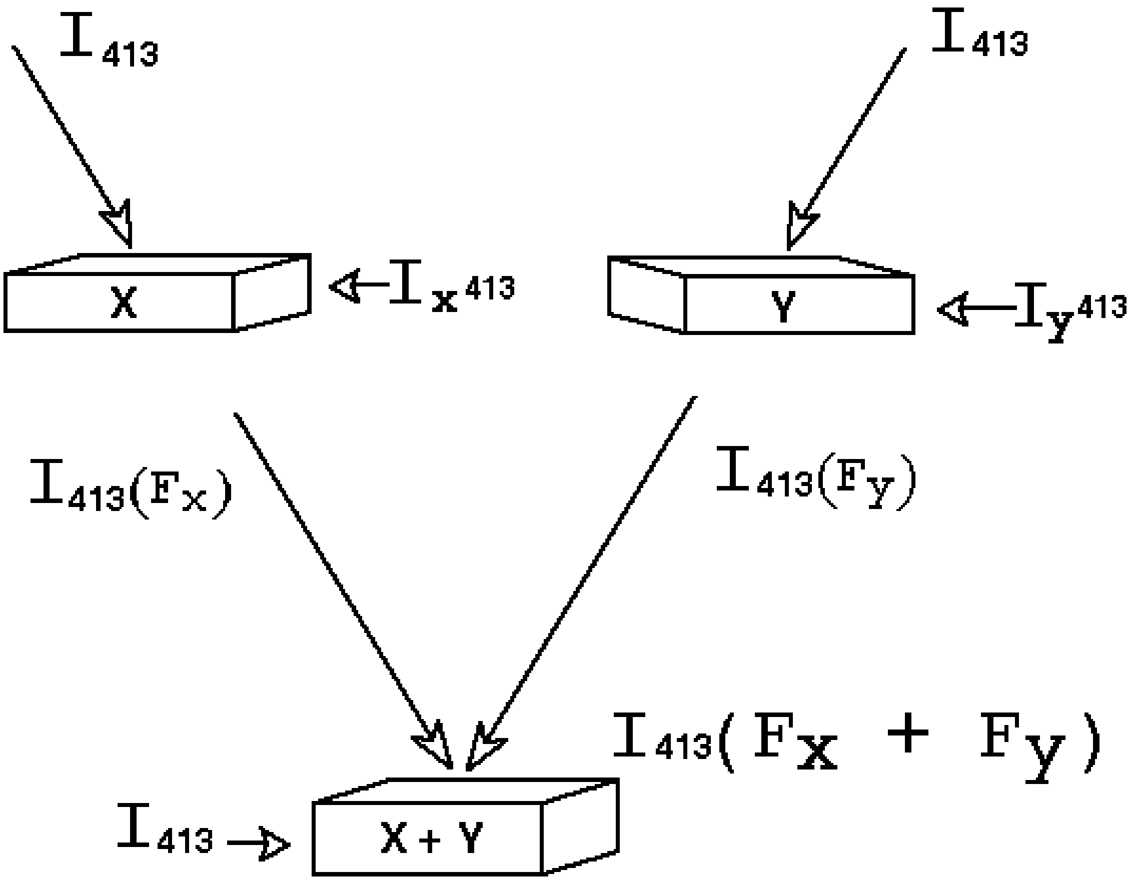

Figure 3.21: The same wavelength setup gives an inverse state result.

depends the amount of the M concentration after the write phase. This transmission will convert the bR to M in the X + Y sample of Figure 3.22. The solution of the addition is represented in the concentration of M in the X + Y sample. Now when it is read with a wavelength of 413nm the answer is in the concentration of bR.

The different wavelength setups are actually a combination of writing with a wavelength of 413nm and reading with a wavelength of 568nm and writing with a wavelength of 568nm and reading with a wavelength of 413nm. Take a look at Figure 3.22; the write and read part is like writing with 413nm and reading with 568nm but the latter part of the experiment (the transmission of the the read and eventually reading out the solutions) is like writing with 568nm and reading with 413nm.

During the investigation of different read and write wavelengths, it was discovered that the ratio of the write over read determines the slope of the line (see Figure 3.19). Also, the read intensities give the altitude of the line (see Figure 3.18).

3.3.2 Results of Adder

The question remains, can the different wavelength setup perform addition? To solve this question a backward solution method is used. Figure 3.23 shows the step that was taken to answer the question of addition. X is written into sample

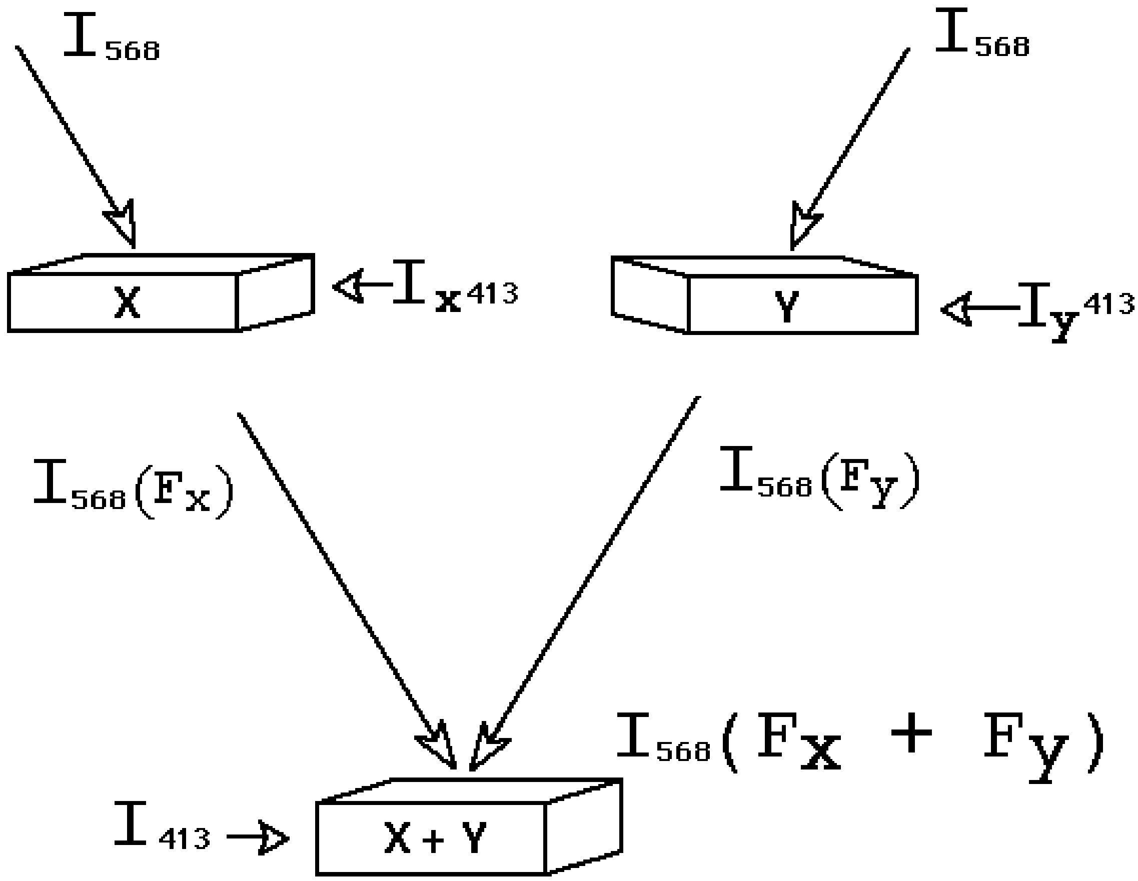

Figure 3.22: The different wavelength setup gives the same state result.

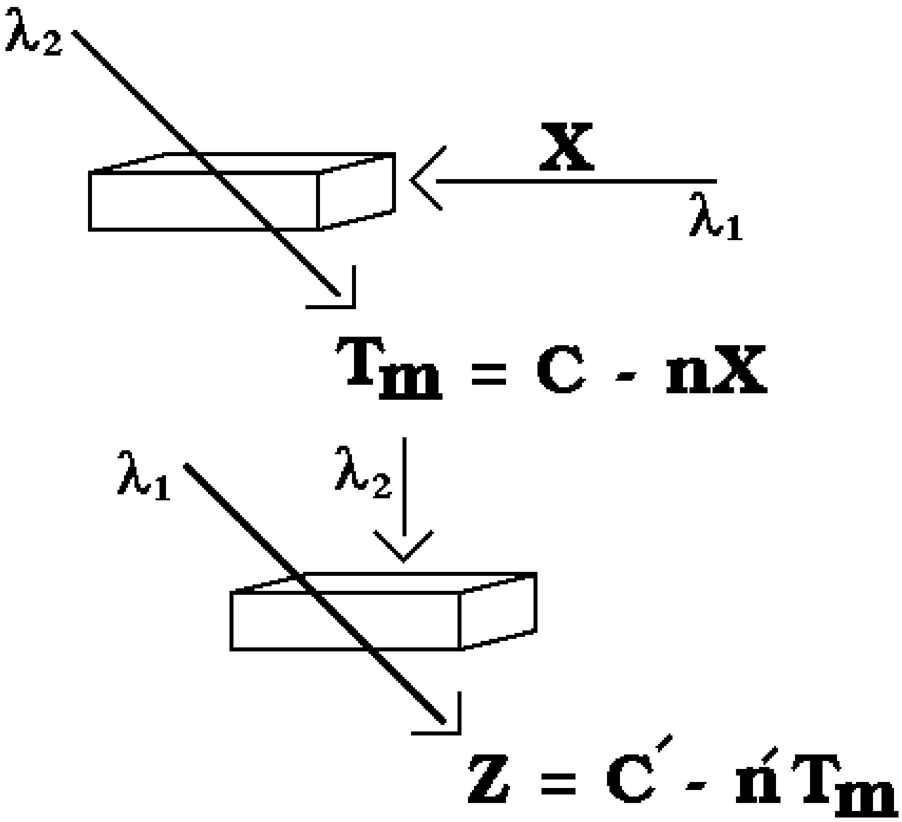

Figure 3.23: The backward setup for solving addition.

A with wavelength λ_1 and a second wavelength, λ_2, is used to read the sample which produce the transmission T_m. T_m is a function of X, n (the slope of the line), and C (the y-intercept). Then T_m is written into sample B and then read with a wavelength, λ_1 which yields Z. Z is a function of T_m, n' (the slope of the line) and C' (the y-intercept). Now it is a substitution to get Z as a function of X (equation 3.1).

$$Z = C' - n'(C - nX) \tag{3.1}$$

What is desired is $Z = X$. This means that X can be encoded into BR and then be read out again. However, when addition is performed overflow has to be taken into account and managed. There are several ways to handle overflow; the method that was used in this case was to cut the input in half from both reads. That way it would never get out of range. Then it can be stated that:

$$\frac{X}{2} = Z = (C' - n'C) + (n'nX)$$

Finally to make the equation true these equations must hold:

$$n'n = \frac{1}{2} \text{ or } n' = \frac{1}{2n}$$

$$C' = n'C \text{ or } C' = \frac{C}{2n}$$

For the initial write and read, the calculated slope and y-intercept is $n = 1.11$ and $C = 300$. The calculated n' and C' is $n' = -0.45$ and $C' = 135$. Finally, the simulation results for n' and C' is $n' = -0.404$ and $C' = 85$.

Chapter 4

Conclusion

4.1 Summary

The different wavelength setup is a better setup that the same wavelength setup for addition. From the data it can be concluded that Bacteriorhodpsin can perform analog field addition. The slopes of the backward solution were within an error range of 10 percent and even though the y-intercept was off a little, it was not so bad that it will serverly hamper the addition.

4.2 Time vs Intensity vs Thickness

As predicted and confirmed with the initial experiments, time, intensity and thickness are directly and indirectly proportional to one another. First, decreasing the time it takes for a molecule to switch states requires more power. However, if too much power is used it is possible to burn up the sample or eradicate the information before reading the output. Also, if the sample is rather thick a longer time is needed to switch states (or the intensity needs to be increased), thereby having an adder that consumes a lot of time.

The data suggest that intensity and thickness are approximately proportional to each other. In fact, the proportion is about a factor of 2. Also the data shows that increasing the sample thickness decreases the transmitted light through the sample.

4.3 Future Work

Even though this work answers some of the questions posed initially, it led to more questions that require research at another level. The next step would be to try these experiments physically and see how they differ from the computational model. The results would provide great insight into the understanding of what BR is doing and what it is capable of doing.

Also, experimenting with the quantum yields, molar extinction coefficient and the M state life span would be useful in discovering the ideal BR that would result in the best adder. So instead of making the experimented work fit the BR, make the BR fit the experiment [15].

Another thing that can be done is to try other computational schemes, such as division, multiplication and subtraction. These are the basic computational concepts that is necessary for the development of a universal field computer.

Bibliography

Bibliography

[1] R. R. Birge. Photophysics and molecular electronic applications of the rhodopsins. *Annual Review of Physical Chemistry*, 41:683–733, 1990.

[2] R. R. Birge. Protein-based optical computing and memories. *Computer*, 23(11):56–67, November 1992.

[3] R. R. Birge. Protein-based computers. *Scientific American*, pages 90–95, March 1995.

[4] S. Chen, A. Lewis, H. Takei, and I. Nebenzahl. Bacteriorhodopsin oriented in polyvinyl alcohol films as an erasable optical storage medium. *Applied Optics*, 30(35):5188–5196, December 1991.

[5] R. R. Birge et al. Nonlinear optical properties of bacteriorhodopsin and protein-based two-photon three-dimensional memories. *Nonlinear Optics*, 3:133–147, 1992.

[6] R. B. Gross, K. C. Izgi, and R. R. Birge. Holographic thin films, spatial light modulators and optical associative memories based on bacteriorhodopsin. In *Proceedings SPIE, International Society for Optical Engeneering*, volume 1662, pages 186–196, 1992.

[7] J. Y. Huang, Z. Chen, and A. Lewis. Second-harmonic generation in purple membrane-poly(vinyl alcohol) films: Probing the dipolar characteristics of the bacteriorhodpsin chromophore in br_{570} and m_{412}. *The Journal of Physical Chemistry*, 93(8):3314–3320, 1989.

[8] B. J. Maclennan. Technology-Independent Design of Neurocomputers: The universal field Computer. In *Proceedings IEEE first International Conference on Neural Networks*, volume 3, pages 39–49, 1987.

[9] B. J. Maclennan. Outline of a theory of massively parallel analog computation. In *poster presentation at IEEE/INNS International Joint Conference on Neural Networks, Washington, D.C.*, volume 2, page 596, June 1989.

[10] B. J. Maclennan. Field Computation: A Theoretical Framework For Massively Parallel Analog Computation; parts I - IV. Technical Report CS–90–100, University of Tennessee, Knoxville, TN, Febuary 1990.

[11] B. J. Maclennan. Flexible Computing in the 21st Century. *Vector Register (Journal of the Institute for Supercomputing Research, Tokyo, Japan)*, 4(3):8–12, 1991.

[12] B. J. Maclennan. Research Issues in Flexible Computing: Two Presentations in Japan. Technical Report CS–92–172, University of Tennessee, Knoxville, TN, September 1992.

[13] B. J. Maclennan. The Emergence of Symbolic Processes From the Subsymbolic Substrate. Technical Report CS–92–159, University of Tennessee, Knoxville, TN, June 1992.

[14] B. J. Maclennan. Continuaous Computation and the Emergence of the Discrete. Technical Report CS–94–227, University of Tennessee, Knoxville, TN, March 1994.

[15] R. Thoma, N. Hampp, C. Brauchle, and D. Oesterhelt. Bacteriorhodopsin films as spatial light modulators for nonlinear-optical filtering. *Optics Letters*, 16(9):651–653, May 1991.

[16] W. J. Tomlinson. Dynamics of photochromic conversion in optically thick samples. *Applied Optics*, 15(3):821–826, March 1976.

Appendix

```
% This is a script file in Matlab.  It loop through different intensities
% and give saturation points.  The graph is made with fraction vs time.
%
% ******************************************************************
% ******************************************************************
% ****************** Beginning of the X+Y module ******************
% ******************************************************************
% Forward Photochemical Rate Constant variables at 413nm for the X+Y module
  PHIbRtM    =  0.64;                % [ no units ]
  EpsbR413   =  15000;               % [ M(-1) cm(-1) ]
  lamda413   =  5.68e-7;             % [ m ]
  Na         =  6.02205e23;          % [ molecules / mole ]
  h          =  6.62618e-34;         % [ J sec ]
  c          =  3.0e8;               % [ m / sec ]
% Reverse Photochemical Rate Constant Formula (at 413nm) ---------------
  PHImtbR    =  0.64;                % [ no units ]
  Epsm413    =  45000;               % [ M(-1) cm(-1) ]

% Forward Photochemical Rate Constant variables at 568nm for the X+Y module
  EpsbR568   =  63000;               % [ M(-1) cm(-1) ]
```

```
% Reverse Photochemical Rate Constant Formula (at 568nm) ---------------

  Epsm568    =  0;                  % [ M(-1) cm(-1) ]

  lamda568   =  5.68e-7;            % [ m ]



% Initial values -------------------------------------------------------

  BRo    = 0.004;            % total concentration of film   [ Moles ]

  Km     = (1/600);          % M thermal decay rate constant [ sec(-1) ]

  Thick  = 0.01;             % total thickness of thin film  [ m ]

  Tn     = 1.0e-4;           % a slice of the thin film      [ m ]

  deltaT = 1.0e-5;           % a small increment of time     [ s ]

  filmS  = (Thick/Tn);       % size of a slice of film       [ m ]


  Tm1    = 0.02;             % total write time              [ s ]

  filmT1 = (Tm1/deltaT);     % number of iteration per slice [ s ]


  Tm2    = 0.005;            % total read time               [ s ]

  filmT2 = (Tm2/deltaT);     % number of iteration per slice [ s ]


  InputI = zeros(1,21);

  Output1I = zeros(1,21);
```

```
% Matrices initialization  1 ---------------------------------------
% *****************************************************************
% ******************* Beginning of module **************************
% *****************************************************************

 M1          = 0.004 * ones(1,filmS);
 bR1         = zeros(1,filmS);

% ------------------------------------ write -----------------------
for Icount = 1:filmT1
  In413i = 0;    %  CHANGE intensity

  for Nslice = 1:filmS
    K413mtbR = (2.3026 * PHImtbR * Epsm413 * lamda413 * In413i )/( Na * h * c);
    K413bRtm = (2.3026 * PHIbRtM * EpsbR413 * lamda413 * In413i )/( Na * h * c);
    deltaM   = deltaT *  ((K413bRtm * bR1(Nslice)) + (-K413mtbR * M1(Nslice))
                    - (Km * M1(Nslice)));
    bR1(Nslice)       =  bR1(Nslice) - deltaM ;           % new bR concentration
    M1(Nslice)        =  M1(Nslice)  + deltaM ;           % new M concentration
    In413i = In413i * exp(-2.3026 * Tn  * (Epsm413 * BRo + (EpsbR413 - Epsm413)
```

```
                    * (bR1(Nslice)/BRo) * BRo));
  end
end

InputI(1) = 0;

% ------------------------------- read ------------------------------
Imatric1b   = zeros(1,filmT2);

for Icount = 1:filmT2
  In568i = 250;    %  CHANGE intensity

  for Nslice = 1:filmS
    K568mtbR   = (2.3026 * PHImtbR * Epsm568 * lamda568 * In568i )/( Na * h * c);
    K568bRtm   = (2.3026 * PHIbRtM * EpsbR568 * lamda568 * In568i )/( Na * h * c)
    deltabR    = deltaT * ((-(K568bRtm * bR1(Nslice))) + (K568mtbR * M1(Nslice))
                    + (Km * M1(Nslice)));
    M1(Nslice)       = M1(Nslice) - deltabR;
    bR1(Nslice)      = bR1(Nslice) + deltabR;
    In568i = In568i * exp(-2.3026 * Tn * (Epsm568 * BRo + (EpsbR568 - Epsm568)
                    * (bR1(Nslice)/BRo) * BRo));
```

```
    end

    Imatric1b(Icount)  = In568i;
  end

  Output4I(1) = sum(Imatric1b)/Icount;
% *******************************************************************
% ******************* End of the  module *****************************
% *******************************************************************

% Matrices initialization  2 ----------------------------------------
% *******************************************************************
% ******************* Beginning of module ****************************
% *******************************************************************

  M2         = 0.004 * ones(1,filmS);
  bR2        = zeros(1,filmS);

% ------------------------------------- write -----------------------

  for Icount = 1:filmT1
```

```
  In413i = 5;    %  CHANGE intensity

  for Nslice = 1:filmS
    K413mtbR = (2.3026 * PHImtbR * Epsm413 * lamda413 * In413i )/( Na * h * c);
    K413bRtm = (2.3026 * PHIbRtM * EpsbR413 * lamda413 * In413i )/( Na * h * c);
    deltaM   = deltaT *  ((K413bRtm * bR2(Nslice)) + (-K413mtbR * M2(Nslice))
                    - (Km * M2(Nslice)));
    bR2(Nslice)       =  bR2(Nslice) - deltaM ;           % new bR concentration
    M2(Nslice)        =  M2(Nslice)  + deltaM ;           % new M concentration
    In413i = In413i * exp(-2.3026 * Tn  * (Epsm413 * BRo + (EpsbR413 - Epsm413)
                   * (bR2(Nslice)/BRo) * BRo));
  end
end

InputI(2) = 5;

% ---------------------------------------------- read -----------------------------

Imatric2b   = zeros(1,filmT2);

for Icount = 1:filmT2
```

```
  In568i = 250;    %  CHANGE intensity


  for Nslice = 1:filmS

    K568mtbR   = (2.3026 * PHImtbR * Epsm568 * lamda568 * In568i )/( Na * h * c);

    K568bRtm   = (2.3026 * PHIbRtM * EpsbR568 * lamda568 * In568i )/( Na * h * c)

    deltabR    = deltaT * ((-(K568bRtm * bR2(Nslice))) + (K568mtbR * M2(Nslice))

                         + (Km * M2(Nslice)));

    M2(Nslice)       = M2(Nslice) - deltabR;

    bR2(Nslice)      = bR2(Nslice) + deltabR;

    In568i = In568i * exp(-2.3026 * Tn * (Epsm568 * BRo + (EpsbR568 - Epsm568)

                     * (bR2(Nslice)/BRo) * BRo));

  end


  Imatric2b(Icount)  = In568i;

end


Output4I(2) = sum(Imatric2b)/Icount;


% ********************************************************************

% ****************** End of the  module ****************************

% ********************************************************************
```

```
% ----------------------  Plotting Write ----------------------------

set (gcf, 'defaultaxescolororder', [1 1 1 ]);
set (gcf, 'defaultaxeslinestyleorder', '-|--|:|-.');

% -------------------------  fraction plot --------------------------
plot (InputI,Output4I)
xlabel ('Input Intensity')
ylabel ('Average Output Transmission');
title('Input vs Average Output Transmission (413-568)');

print try10                %  Output plot name
legend off;

% -------------------------------------------------------------------
```

Vita

Quentin A. Browne grew up on St. Croix, one of the United States Virgin Islands. He received his high school education from St. Croix Central High school. He received his Bachelor of Science degree in Physics from Stillman College at Tuscaloosa, Alabama. He entered the University of Tennessee at Knoxville in August 1993, and received a Master of Science degree in Computer Science in December 1996. He has interned with AT&T Bell Labs for several summers during his academic career.